

Chapter 9

Coating Performance

9.1 Corrosion Protection Performance of Organic Coatings

9.1.1 Definitions and Methods

There is no single parameter or property that can characterise the corrosion protection capability or performance of coating systems. It is rather a mixture of parameters that must be considered. The same problem applies to testing methods. Standard parameters for the assessment of the behaviour of corrosion protective coatings are summarised in Fig. 9.1. Basically, the performance of undamaged and artificially injured coating systems is evaluated. Examples for the effects of different surface preparation methods on the corrosion at artificial scribes are provided in Fig. 9.2. It can be seen that the performance was worst for the untreated sample and best for the blast cleaned sample. Samples prepared with power tools showed moderate performance.

Failure evaluation of coating systems involves the following three conditions (ISO 4628-1):

- failure size;
- failure distribution;
- failure intensity.

Some authors tried to generalise results of visual inspection methods. Vesga et al. (2000) introduced a *KIV*-value (Constant-Inspection-Visual) for the assessment of primers applied to substrates prepared with different surface preparation methods. The *KIV*-value reads as follows:

$$KIV = 100 - \sum (\text{corrosion products} + \text{blister size} + \text{blister density}) \quad (9.1)$$

The criteria for the assessment of the three performance parameters are listed in Table 9.1. The term “corrosion products” corresponds to the degree of rusting according to ISO 4628-2, whereby “blister size” and “blister density” correspond to the degree of blistering according to ISO 4628-3. The higher the *KIV*-value, the better the coating performs. A freshly applied defect-free coating at $t = 0$ has a value

Fig. 9.1 Coating performance assessment parameters according to ISO 4628

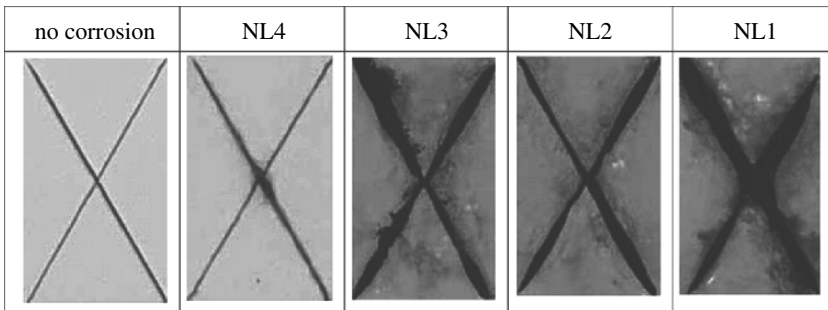
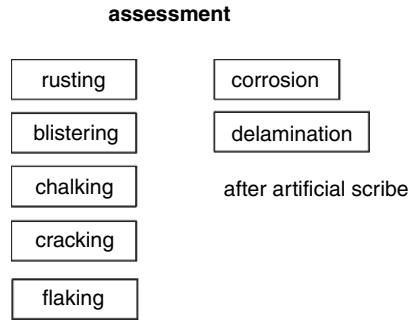


Fig. 9.2 Effects of surface preparation on underscribe corrosion (Kim et al., 2003). NL1 – untreated; NL2 – grinding (light rust removed); NL3 – grinding (rust completely removed); NL4 – dry blast cleaning

of $KIV = 100$. A coating with a value of $KIV = 36$ shows the worst performance. Figure 9.3 illustrates results of this procedure: KIV -values are plotted against the testing duration as functions of different surface preparation methods. The values for KIV decrease, as expected, with an increase in testing time, and they also show a dependence on the surface preparation method, at least for long exposure times.

Artificially injured coatings play a role for laboratory tests, such as for the neutral salt spray tests. In these cases, the artificial scribes simulate mechanical damage to the coating systems. Test duration depends on the corrosivity of the environment the coatings have been designed for. Examples are listed in Table 9.2. For certain

Table 9.1 Criteria for degree of blistering and degree of rusting (ISO 4628-1)

Criterion	Defect quantity	Defect size
0	No (resp. not visible) defects	Not visible at 10 × magnification
1	Very few defects	Visible only at 10 × magnification
2	Few defects	Just visible with unaided eye
3	Moderate number of defects	Clearly visible with unaided eye (up to 0.5 mm)
4	Considerable number of defects	Range between 0.5 and 5.0 mm
5	High number of defects	Larger than 5.0 mm

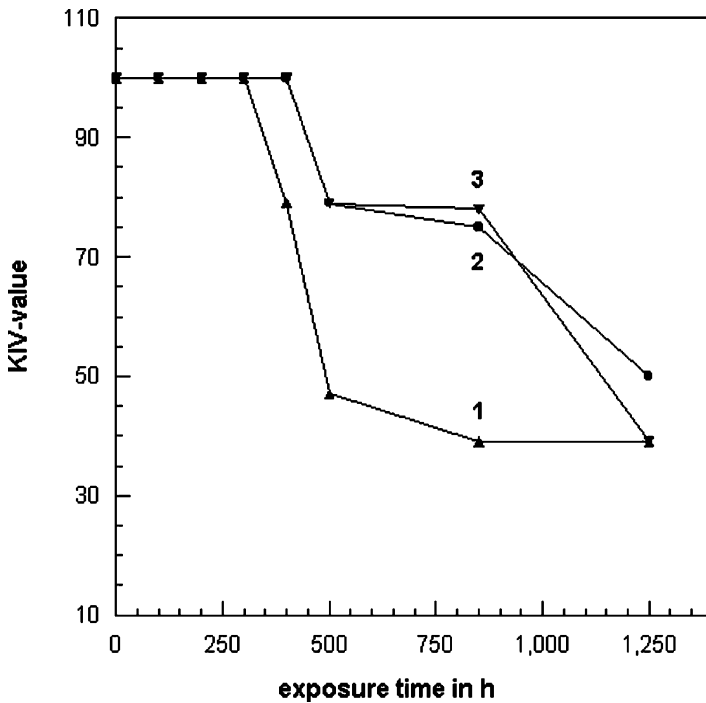


Fig. 9.3 Relationship between KIV and surface preparation methods (Vesga et al., 2000). Preparation methods: 1 – wet blast cleaning; 2 – wet blast cleaning with inhibitor; 3 – dry blast cleaning

application, for example for the use of coatings for offshore structures, special test regimes have been developed. An example is displayed in Fig. 9.4.

The methods for the damage and failure assessment are visually determined, although certain parameters, namely degree of rusting and degree of blistering, can be alternatively assessed by more objective methods, such as computerised image analysis methods (Momber, 2005b). Examples are provided in Fig. 9.5.

Table 9.2 Relationships between corrosivity and test conditions for coatings according to ISO 12944-6 (Projected coating durability: >15 years)

Corrosivity category ^a	Test duration in hours			
	Chemical resistance	Water immersion	Water condensation	Neutral salt spray
C2	–	–	120	–
C3	–	–	240	480
C4	–	–	480	720
C5-I	186	–	720	1,440
C5-M	–	–	720	1,440
Im1	–	3,000	1,440	–
Im2	–	3,000	–	1,440
Im3	–	3,000	–	1,440

^a Defined in ISO 12944-1




day 1	day 2	day 3	day 4	day 5	day 6	day 7
UV/condensation — ISO 11507			salt spray — ISO 7253			low-temp. exposure at (-20±2) °C
						

Fig. 9.4 Coating performance testing regime for offshore applications according to ISO 20340

Bockenheimer et al. (2002) performed investigations into the curing reactions of epoxy systems applied to aluminium, and they found different degrees of conversion of epoxy groups on the pretreated surfaces. Results of this study are plotted in Fig. 9.6. It can be seen that blast cleaning notably reduced the final degree of conversion of the epoxy groups. A distinct effect of the abrasive type could also be noted. The authors could further show that blast cleaned surfaces not only influenced the formation of the network structure in the near-interphase region, but also far from substrate.

9.1.2 Coating Performance After Blast Cleaning

9.1.2.1 Introduction

Systematic investigations about the effects of different surface preparation methods on the performance of organic coatings are provided by Allen (1997), Morris (2000), Momber et al. (2004) and Momber and Koller (2005, 2007). The first three authors mainly dealt with the adhesion of organic coatings to steel substrate; their results are presented in Sect. 9.2.

Vesga et al. (2000) utilised the *KIV*-criterion mentioned in Sect. 9.1.1. Results are provided in Fig. 9.3. For comparatively short exposure times ($t < 300$ h) and long exposure times ($t = 1,250$ h), this parameter was insensitive to surface preparation methods. At moderate exposure times, primer performance depended notably on surface preparation method. Primers applied over wet blast cleaned substrates deteriorated very quickly after a threshold time level was passed. The decrease in the resistance of primers applied over dry blast cleaned substrates was moderate after the threshold exposure time was exceeded. The addition of an inhibitor to the water for wet blast cleaning did not notably improve the performance of primers for longer exposure times. An inhibitor improved the situation basically for moderate exposure times only. Vesga et al. (2000) found that electrochemical impedance spectroscopy (EIS) can be utilised for the evaluation and assessment of the protective performance of organic coating systems. Pore resistance values measured on primers applied over steel substrates prepared with dry blast cleaning and wet blast cleaning showed the same qualitative trend as the *KIV*-values.

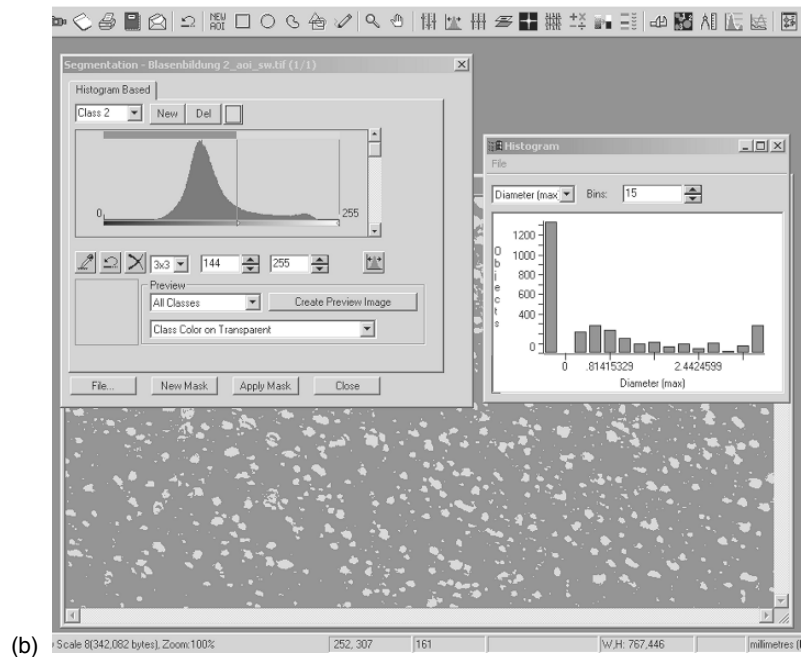
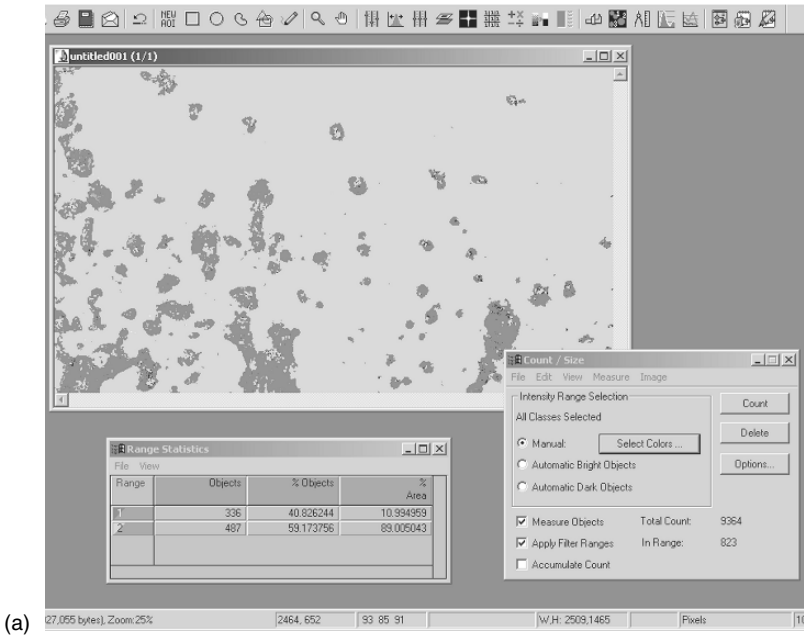


Fig. 9.5 Assessment of coating damaged based on digital image processing (Images: Muehlhan AG, Hamburg). (a) Degree of rusting; (b) Degree of blistering

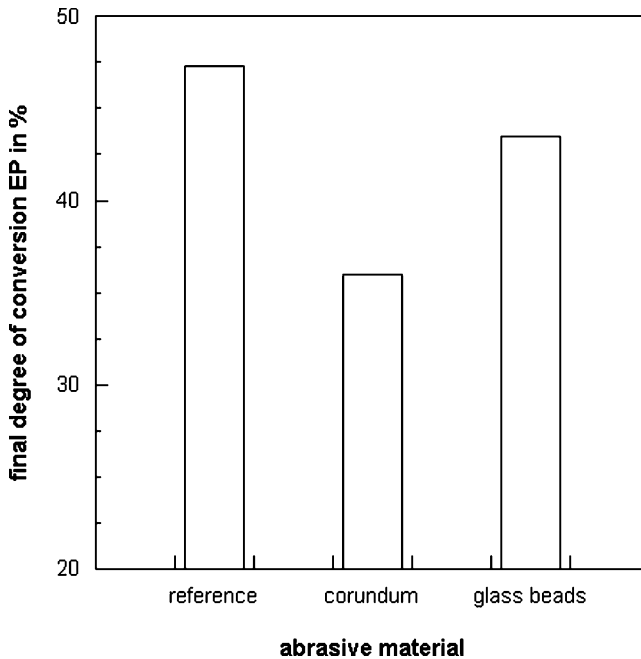


Fig. 9.6 Final degree of conversion of epoxy groups for 2 μm films on aluminium (Bockenheimer et al., 2002)

9.1.2.2 Coating Delamination

Results of measurements of coating delamination at artificial scribes were reported by several authors (Haagen et al., 1990; Van der Kaaden, 1994; Pietsch et al., 2002; Momber and Koller, 2005, 2007; Claydon, 2006). Some results are displayed in Fig. 9.7. Coatings applied to wet blast cleaned substrates showed the lowest delamination rate, whereas coatings applied to dry blast cleaned substrates performed worst. These results were attributed to substrate contamination due to broken abrasive debris. If blast cleaning was compared with manual surface preparation, delamination widths were larger for blast cleaned substrates, at least for epoxy coatings with zinc phosphate fillers subjected to wetting–drying cycles (Pietsch et al., 2002). Results of respective tests are shown in Figs. 9.8 and 9.9. Delamination of zinc phosphate primers at the artificial scribe on blast cleaned substrate occurred due to cathodic delamination. Using zinc dust primers, especially the edges of the scribe were cathodically protected by the anodic dissolution of zinc. Because of the formation of zinc oxides, increasing exposure time can lead to a deactivation of zinc dust and a progression of the corrosion process. Haagen et al. (1990) investigated the delamination of coatings on non-rusted substrates, and they found that blast cleaned surfaces were superior over mechanically ground surfaces. Some of their results are listed in Table 9.3. Figure 9.10 illustrates the effects of abrasive types on coating delamination. The coatings tested showed worse performance over shot

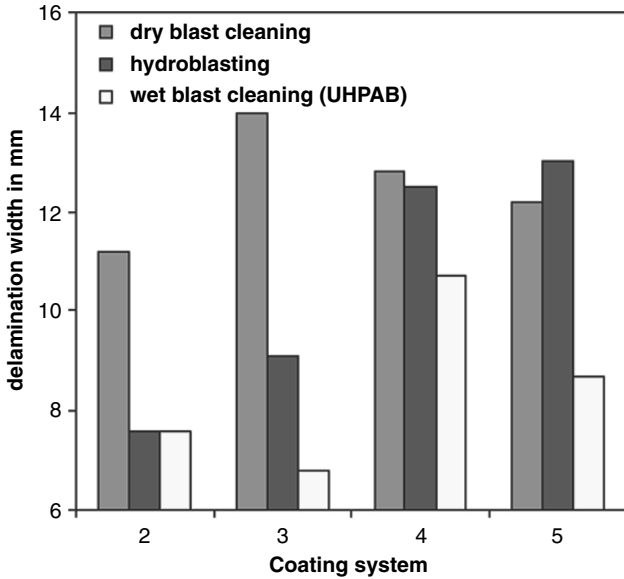


Fig. 9.7 Delamination of organic coatings for different surface preparation methods (Momber and Koller, 2005)

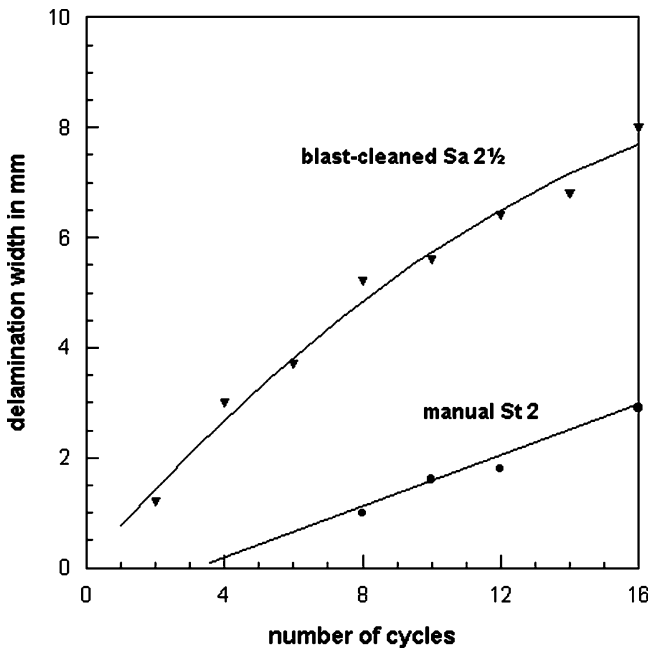


Fig. 9.8 Surface preparation influence on delamination of organic coatings at artificial scribe (Pietsch et al., 2002). Coating: epoxy/polyurethane; Primer: epoxy/zinc-phosphate

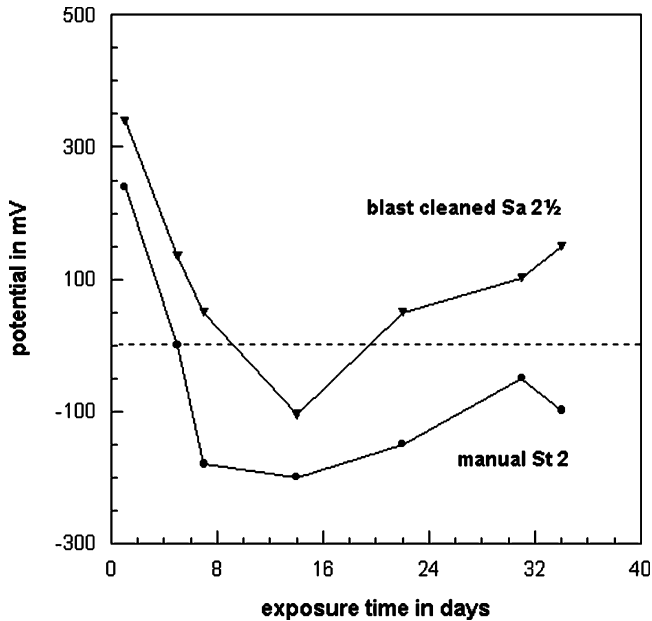


Fig. 9.9 Surface preparation method effects on electric potential below an intact coating (Pietsch et al., 2002). Primer type: zinc dust based primer

blasted steel compared with coatings applied to grit blasted steel during a cyclic corrosion test. If a salt spray test was considered, both abrasive types delivered comparative results. Van der Kaaden (1994) performed a comparative study into the performance of organic coating systems applied to dry blast cleaned and wet blast cleaned steel substrates. The hot-rolled substrates were pre-rusted. Results of this study are listed in Table 9.4. The results reveal the tight relationships between surface preparation method, testing regime, coating type and delamination width. Whereas the wet blasting version with the larger water flow rate (7.0 l/min) showed the best results for the chlorinated rubber in the salt spray test, it performed

Table 9.3 Effects of surface preparation method and test solution on the delamination of coatings after salt spray tests (Haagen et al., 1990), Coating: 2-pack epoxy with micaceous iron ore

Test solution	Delamination in mm	
	Polished	Blast cleaned
NaCl (0.117%)	2–3	2
NaCl (saturated)	4–5	0.5–1
NaCl (5%)	Ca. 11	Ca. 5
NH ₄ NH ₃ (3.2%)	Ca. 1	0
NH ₄ NH ₃ (0.85%)	5–7	2–3
NH ₄ Al(SO ₄) ₂	2–3	0
NH ₄ Cl (2.14%)	0.5	0
CaCl ₂ (2.8%)	1–2	0

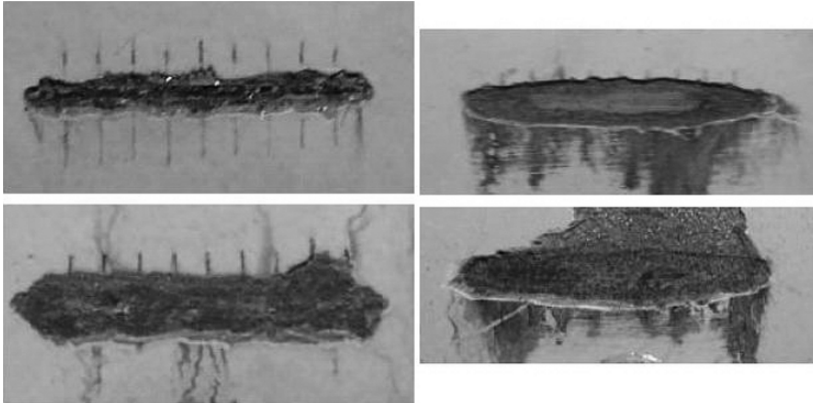


Fig. 9.10 Effects of blast cleaning method on delamination of zinc epoxy primers at an artificial scribe (Claydon, 2006). Upper images: dry blast cleaning with grit; Lower images: dry blast cleaning with shot. Left: after cyclic corrosion test; right: after salt spray test

worst for the high-solid epoxy in the seawater test with cathodic protection. The results for the tests with cathodic protection are of special interest. If the results for chlorinated rubber, obtained during the seawater test, are considered, the preferred surface preparation method would be wet blast cleaning with a low water volume (1.6l/min). As far as cathodic protection was added, the preferred surface preparation method would be wet blast cleaning with a high volume of water (7.0l/min). The opposite trend could be recognized if high-solid epoxies were applied to the blast cleaned surfaces.

Emrich (2003) investigated the delamination of adhesive bonds in aluminium (AlMg₃) samples. He subjected the samples to a salt spray test over a period of

Table 9.4 Delamination of organic coatings at an artificial scribe (Van der Kaaden, 1994)

Preparation method	Coating system	Delamination in mm			
		Sea water (1 year)	Sea water with cathodic protection (1 year)	Artificial rain water (1 year)	Salt spray test (3,000 h)
Dry blast cleaning	Chlorinated rubber	1.4	814.9	76.1	9.5
	Vinyl/tar	2.5	7.9	55.6	6.0
	Coal tar/epoxy	0.0	0.0	59.1	8.5
	High-solid epoxy	13.3	19.4	65.8	5.5
Wet blast cleaning (1.6 l/min)	Chlorinated rubber	1.2	831.3	77.3	8.0
	Vinyl/tar	0.0	0.0	61.0	6.8
	Coal tar/epoxy	0.0	0.0	46.1	8.3
	High-solid epoxy	13.3	30.0	56.9	4.5
Wet blast cleaning (7.0 l/min)	Chlorinated rubber	8.6	703.8	81.3	6.3
	Vinyl/tar	0.0	0.0	110.1	5.3
	Coal tar/epoxy	0.0	0.0	63.8	8.9
	High-solid epoxy	3.9	43.8	20.3	6.0

2,000 h, and he noted a severe delamination of the adhesive on substrates which were blast cleaned with corundum ($p = 0.6 \text{ MPa}$). The delamination was much more severe than delaminations estimated for samples where the substrates were degreased with acetylene. Samples with substrates that were treated by pickling did not show any delamination. If an accelerated corrosion test (6 h in a 5% NaCl solution, subjected to an external current) was applied to the samples, the ranking was different. The samples with the degreased substrates exhibited the most severe delamination, followed by the blast cleaned samples. The best performance was again shown by the samples prepared with pickling.

9.1.2.3 Degree of Rusting

Measurements of the degree of rusting for paints applied to substrates prepared with different surface preparation methods were performed by Grubitsch et al. (1972) and Kogler et al. (1995). Results of the latter authors are displayed in Fig. 1.4. Figure 9.11 shows the effects of different abrasive materials on the degree of rusting of coated (zinc dust) steel panels. There exists the following power relationship between exposure time and degree of rusting:

$$\text{DR} \propto t_E^{k_R} \quad (9.2)$$

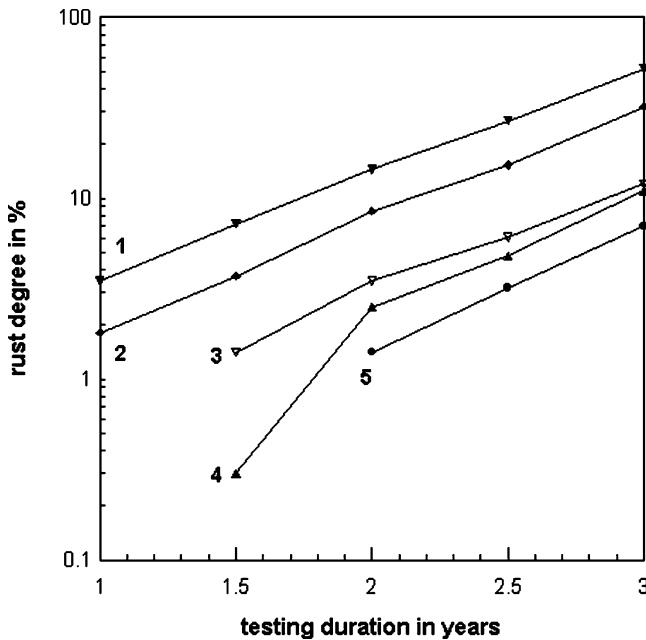


Fig. 9.11 Relationship between ageing kinetics and abrasive materials (Grubitsch et al., 1972). Abrasive materials/method: 1 – slag; 2 – quartz; 3 – aluminium oxide; 4 – steel grit; 5 – etching

Table 9.5 Ageing kinetics parameter in (9.2) for different abrasive materials (Grubitsch et al., 1972)

Abrasive type/method	Grain size in mm	Parameter k_R
Quartz	1.0–2.0	2.6
Corundum	0.8–1.0	–
Slag	1.0–2.0	2.4
Steel grit	0.8–1.0	–
Etching with H ₂ SO ₄	–	–

This relationship could be exploited to describe the kinetics of ageing of a coating system. The power exponent k_R depended on abrasive material type. Values for this parameter are provided in Table 9.5. It can be seen that not only the type of abrasive material determined the ageing kinetics, but also its fineness.

Further results are listed in Table 9.6 where the failure times of two coating systems are listed. The failure time was defined as the time when the first rusting was visible on the coatings. Failure time strongly depended on the abrasive type. For the alkyd paint, for example, failure occurred after 3 months if aluminium oxide was used, but the failure time could be delayed up to 114 months when wet sand was used as an abrasive material. For the acrylic paint, the trend was opposite. Here, the coating applied to the substrate that was blast cleaned with aluminium oxide, showed the best performance.

9.1.2.4 Degree of Blistering

The degree of blistering of organic coatings is sensitive to the type of surface preparation. A systematic study on this issue was undertaken by Kim et al. (2003). Deterioration curves for a coating system, based on the results of long-term blistering tests (251 days) on artificially injured samples, are plotted in Fig. 9.12. Blistering was most severe for the untreated steel and least severe for the blast cleaned substrate. Blast cleaning was more efficient than power tool cleaning. The general relationship

Table 9.6 Effects of abrasive material type on failure times of organic coatings (Boocock, 1992)

Abrasive material	Failure time in months	
	Alkyd paint	Acrylic latex paint
Dry sand	101	114
Wet sand	114	38
Steel shot (S-280)	75	16
Steel grit (G-12)	89	38
Coal slag (coarse)	68	16
Coal slag (fine)	3	–
Staurolite	89	38
Flint	89	94
Copper/coal slag	89	114
Aluminium oxide	3	>126

Surface preparation grade: SP 10 for all samples

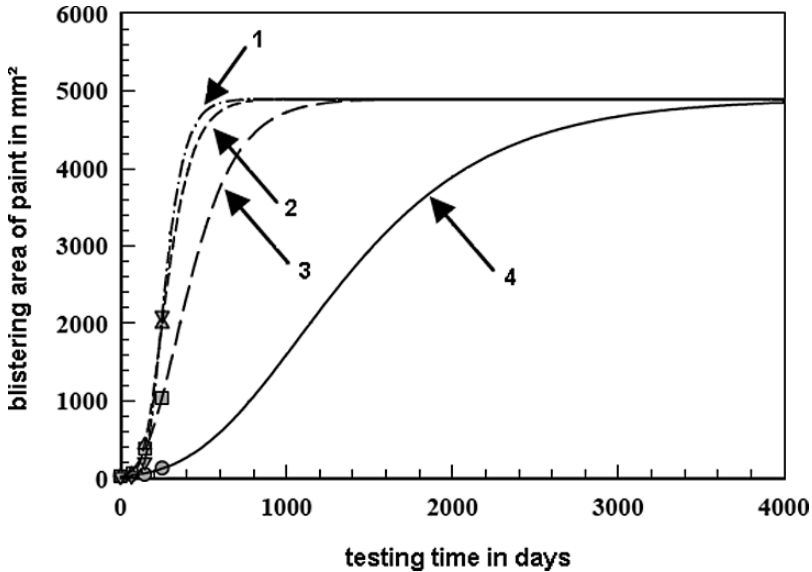


Fig. 9.12 Effects of surface preparation methods on the blister formation kinetics (Kim et al., 2003). Preparation method: 1 – no cleaning; 2 – grinding (light rust removed); 3 – grinding (rust completely removed); 4 – blast cleaning

between exposure time and degree of blistering is essentially equal to (9.2), whereby the power exponent depended on the surface preparation method.

9.2 Adhesion and Adhesion Strength

9.2.1 Definitions and Measurement

9.2.1.1 Definitions

According to Bullett and Prosser (1972) “the ability to adhere to the substrate throughout the desired life of the coatings is one of the basic requirements of a surface coating, second only to the initial need to wet the substrate.” Adhesion bases on adhesive forces that operate across the interface between substrate and applied coating to hold the paint film to the substrate. These forces are set up as the paint is applied to the substrate, wets it and dries. The magnitudes of these forces (thus, the adhesion strength) depend on the nature of the surface and the binder of the coating. Five potential mechanisms cause adhesion between the surfaces of two materials (see Fig. 9.13):

- physical adsorption;
- chemical bonding;
- electrostatic forces;

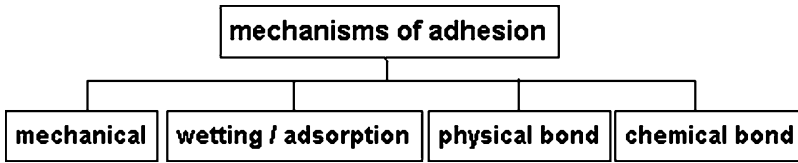


Fig. 9.13 Mechanisms of adhesion

- diffusion;
- mechanical interlocking.

In the mechanical interlocking mechanism, the macroscopic substrate roughness provides mechanical locking and a large surface area for bonding; the paint is mechanically linked with the substrate. Adhesive bonding forces could be categorised as primary and secondary valency forces as listed in Table 9.7. Adhesion depends on numerous factors, including those summarised in Fig. 9.14. It is instructive to note that the adhesion is to a certain amount a “test parameter” depending on test conditions and specifications. Adhesion values get a comparative meaning only if assessed under equal test conditions.

9.2.1.2 Adhesion Measurement

Adhesion between substrate and organic coating can be evaluated on site by different methods, including the following:

- pull-off testing; for coating dry film thickness DFT > 250 μm;
- X-cut testing;
- cross-cut testing; for coating dry film thickness DFT < 250 μm;
- falling ball impact;
- penknife disbondment.

For adhesive bonds, metallic coatings and ceramic coatings, other, more advanced testing methods (peel tests, indentation debonding tests, scratch tests, beam-bending tests, etc.) are available; a recent extensive review was delivered by Lacombe (2006). Berndt and Lin (1993) and Lin and Berndt (1994) provided a review about methods used to define and measure the adhesion of coatings or deposits formed by thermal spraying; their review included tensile adhesion test, double cantilever beam test, scratch test and bending test.

The pull-off test delivers quantitative information about the strength of the bond (usually given in N/mm², respectively MPa), while the picture of the rupture provides information about the weakest part of the system. The adhesion strength (referred to as pull-off strength if measured with the pull-off test) is the relationship between applied force and loaded cross-section:

$$\sigma_A = \frac{F_A}{A_A} \tag{9.3}$$

Table 9.7 Bonding forces and binding energies (Hare, 1996)

Force	Type	Description	Example	Binding energy in kcal/mole
Ionic	Primary valency	Bonding formed by transfer of valency electrons from the outer shell of an electron-donating atom into outer shell of an electron-accepting atom, to produce a stable valency configuration in both.	Metal salts	150–250
Covalent	Primary valency	Bonding formed when one or more pairs of valency electrons are shared between two atoms.	Most organic molecules	15–170
Co-ordinate	Primary valency	Covalent type bond where both of shared pair are derived from one of the two atoms.	Quaternary ammonium compounds	100–200
Metallic	Primary valency	Bonding in bulk phase of metals between positively charged metallic ions and the electron cloud in the lattice points of the structure.	Bulk metals	27–83
Hydrogen bonding	Secondary valency	Forces set up between the unshared electrons on a highly electronegative atom on one molecule and the weak positive charge from the 'exposed' proton of a hydrogen atom.	Water	<12
Dispersion	Secondary valency	Weak forces in all molecules that are associated with temporary fluctuations in electron density caused by the rotation of electrons around atomic nuclei.	Most molecules	<10
Dipole	Secondary valency	Intermolecular forces set up between weak and electronegative charge on one polar molecule and electropositive charge on a second polar molecule.	Polar organics	<5
Induction	Secondary valency	Very weak dipole-like forces between non-polar molecules set up by weak dipoles induced by the proximity of other strongly polar molecules.	Non-polar organics	<0.5

Frequently, adhesion strength is given in kN, which is the unit of a force. Obviously, this information is useful only if the loaded cross-section is known. It can, however, be used as a comparative measure if the loaded cross-section is a constant, exactly defined value.

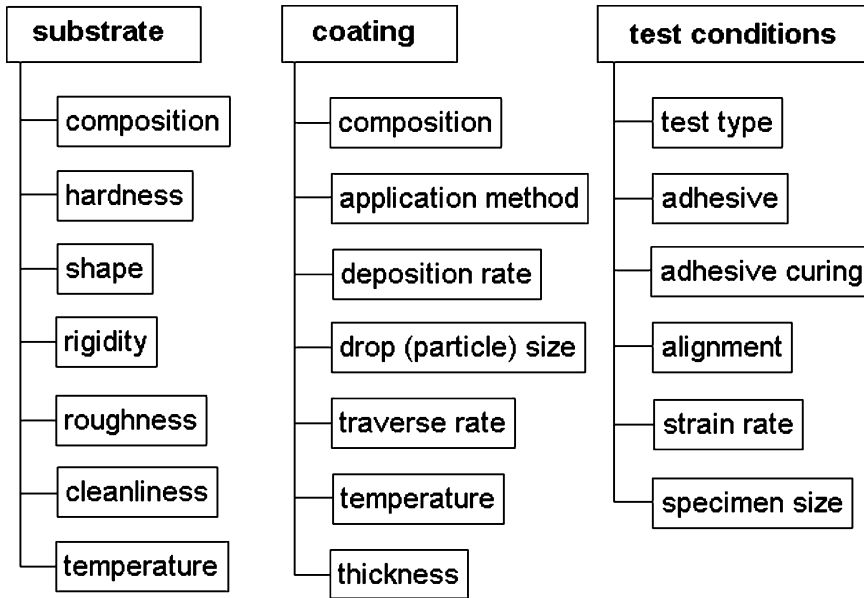


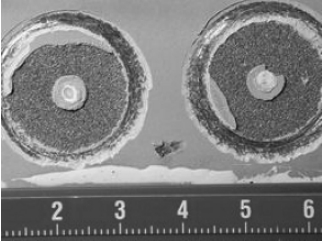
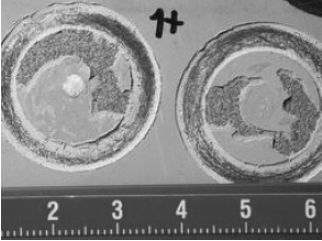
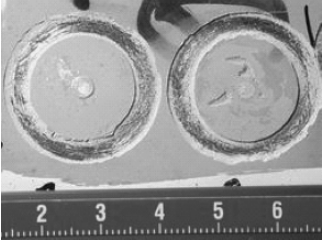
Fig. 9.14 Influence factors on the adhesion of coatings to steel substrates (James, 1984)

Typical failure types to be observed during pull-off tests are either adhesive failure (substrate-coating), cohesive failure (internal coating failure) or mixed adhesive-cohesive failure. More detailed designation is mentioned in Table 9.8. Strictly spoken, a plain adhesion failure will never occur in a coating-substrate system. This restriction is reinforced by XPS (X-ray photoelectron spectroscopy) measurements performed by van den Brand et al. (2004) and Watts and Dempster (1992), who found traces of polymeric material on the substrate surface of a metal-polymer interfacial fracture, which appeared to be a purely adhesive failure from an optical examination.

Time and environmental conditions are important parameters in the experimental estimation of adhesion parameters. Because the hardening of coating materials is a reaction kinetics process, the bond between substrate and coating, respectively adhesive, is a time-domain process. Emrich (2003), for example, measured the shear strength of an aluminium-adhesive joint subjected to a salt spray test. The aluminium substrate (AlMg₃) was blast cleaned with corundum ($p = 0.6$ MPa). Prior to the salt spray exposure, the shear strength had a value of 15.5 MPa. After a period of 2,000 h, however, the shear strength had dropped down to a value of 4.5 MPa only. This author could also show that the adhesion of the adhesive was extremely sensitive to ageing when the adhesive was applied to blast cleaned substrates. Other surface preparation methods, namely degreasing with acetylene and pickling, were much less sensitive to ageing effects. Further experimental information on these aspects is available in the literature, and it will be discussed in the following sections.

Desired adhesion depends on the certain case of application. The US Navy, for example, has defined a general minimum pull-off strength of $\sigma_A = 3.4$ MPa

Table 9.8 Failure modes after pull-off testing of organic coatings (Momber and Koller, 2005)

Method	Failure figure	Failure type ^a
Dry blast cleaning		100% A/B
Hydroblasting		60% B, 40% A/B (left) 70% B, 30% A/B (right)
Wet blast cleaning (Ultra-high pressure abrasive blasting)		100% B

^aA/B-adhesive failure coating/substrate

B-cohesive failure coating

measured per ASTM D4541 (Kuljan and Holmes, 1998). Demands for marine constructions are listed in Table 9.9.

9.2.2 Adhesion of Coatings and Adhesives to Metal Substrates

Sobiecki et al. (2003) conducted a study into the effects of surface preparation methods on the structure of the interfacial zone between steel substrate and a tungsten carbide coating. They found that the porosity in the interfacial zone depended on the surface preparation prior to the coating process. The porosity was lowest for grinding and highest for blast cleaning.

Several systematic studies were performed to estimate the adherence of coating systems to steel panels prepared by different methods. Long-term tests in salt water were performed by Allen (1997) and Morris (2000). These studies included hand wire brushing, needle gunning, hydroblasting and blast cleaning. The

Table 9.9 Critical adhesion strength values for some coatings (Norsok, 2004); using equipment according to ISO 4624, and carry out test when coatings are fully cured

Coating type/Application	DFT in μm	Pull-off strength in MPa (absolute minimum)	Failure mode
Thermally sprayed aluminium (or alloys)	200	7.0	–
Thermally sprayed zinc (or alloys of zinc)	100	5.0	Cohesive
Potable water tanks	–	5.0	–
Tanks for crude, diesel and condensate	–	5.0	–
Process vessels (<0.3 MPa, <75°C)	–	5.0	–
Process vessels (<7 MPa, <80°C)	–	5.0	–
Process vessels (<3 MPa, <130°C)	–	5.0	–
Vessels for storage of methanol, etc.	–	5.0	–
Fire protection (cement based)	–	2.0	–
Fire protection (epoxy based)	–	5.0	–

results, listed in Tables 9.10 and 9.11, illustrated the complex relationships between preparation methods and applied coating systems. Cross-cut, measured after 36 months, was almost independent on the preparation method for many epoxy coatings; exceptions were coal tar epoxy and pure epoxy tank lining, where wire brushing and needle gunning showed worse results compared to hydroblasting and blast cleaning. Penknife disbondment and impact resistance, both measured after 24 months, showed worst results for the mechanical methods (especially for the wire brushing). Impact resistance was more a function of the coating system than of the preparation method; thus, blast cleaned substrates were, on the whole, only slightly superior to manual preparation under the conditions of the impact testing. Regarding the pull-off strength, measured with a commercial adhesion tester, blast cleaning methods were superior to mechanical methods. Some results are shown in Fig. 9.15. There was a certain trend for the blast cleaning methods that pull-off adhesion increased with time. Under simulated ballast tank conditions, coatings applied to blast cleaned surfaces performed far better than coatings applied to mechanically prepared substrates, and equal to those on hydroblasted surfaces. It was observed that paint failure type was often a mixture of cohesive and adhesive failures, and the appearance of the certain mode was denoted in percent (see Table 9.8). However, as shown in Tables 9.10 and 9.11, substrate failure (denoted “S”) and coat detachment occurred usually from mechanically prepared surfaces, whereas glue failure (denoted “G”) and inter-coat failure (denoted “I”) were the principal failure mode on most of the blast cleaned and hydroblasted surfaces.

Björgum et al. (2007) investigated the adhesion of repair coating systems for off-shore applications. Pre-rusted steel panels were cleaned with blast cleaning, power tooling and waterjetting. After an accelerated ageing test, the adhesion between coatings and steel substrates was measured with a pull-off device. Although the authors found deviations in the pull-off strength for the different surface preparation methods, these differences were statistically insignificant.

Tests on contaminated substrates showed that the level of dissolved salts affected value and type of adhesion of coatings to substrates. With zero contaminants, the mode of failure was cohesive within the primer coat. As the salt level increased,

Table 9.10 Results of comparative adhesion tests on ballast tank coatings (Allen, 1997)

Method	Adhesion parameter		
	Falling ball impact ^a	Pull-off strength in MPa ^b	Penknife disbondment in mm
Epoxy coating (solvent-less)			
Wire brushing	2	2.8/S	6
Needle gunning	1	2.8/S	5
Hydroblasting (Dw2)	0	6.9/G	0
Hydroblasting (Dw2 FR)	4	3.4/G	0
Hydroblasting (Dw3)	0	3.4/G	0
Hydroblasting (Dw3 FR)	0	4.1/G	0
Blast cleaning (Sa 2½)	1	5.5/G	0
Coal tar epoxy			
Wire brushing	4	2.1/S	10
Needle gunning	3	2.4/S	7
Hydroblasting (Dw2)	0	5.2/I	0
Hydroblasting (Dw2 FR)	2	6.9/I	0
Hydroblasting (Dw3)	0	6.9/I	0
Hydroblasting (Dw3 FR)	2	6.9/I	0
Blast cleaning (Sa 2½)	1	6.6/I	0
Epoxy system			
Wire brushing	2	2.1/S	5
Needle gunning	2	2.8/S	3
Hydroblasting (Dw2)	2	6.9/G	0
Hydroblasting (Dw2 FR)	0	5.5/G	0
Hydroblasting (Dw3)	0	5.2/G	0
Hydroblasting (Dw3 FR)	0	6.9/G	0
Blast cleaning (Sa 2½)	0	5.5/G	0
Glass flake epoxy			
Wire brushing	2	2.8/S	5
Needle gunning	1	4.1/S	3
Hydroblasting (Dw2)	1	6.9/G	0
Hydroblasting (Dw2 FR)	4	5.2/G	0
Hydroblasting (Dw3)	0	3.4/G	0
Hydroblasting (Dw3 FR)	0	5.5/G	0
Blast cleaning (Sa 2½)	0	6.9/G	0

FR flash rust; Dw surface cleanliness according to STG 2222

^a0 = no cracking, no detachment; 1 = slight cracking, no detachment; 2 = slight cracking and detachment; 3 = moderate cracking, no detachment; 4 = moderate cracking, slight detachment

^bFailure mode: G = glue, I = intercoat, S = substrate

progressively less primer remained adhered to the steel surface. At higher contamination level, there was a change from mixed to totally adhesive failure of the primer (Allan et al., 1995). Baek et al. (2006) reported a notable decrease in pull-off strength if the steel substrate was contaminated with chlorides. The drop in adhesion was very pronounced if a chloride concentration of 7 µg/cm² was exceeded.

Kaiser and Schulz (1987) performed cross-cut adhesion tests on coatings applied to zinc surfaces. If the samples were degreased only, the cross-cut adhesion was very low. The adhesion notably improved if the samples were blast cleaned with coal

Table 9.11 Results of comparative long-term adhesion tests after 12, 24 and 36 months (Morris, 2000)

Method	Cross-cut in mm			Impact resistance ^a			Pull-off strength in MPa ^b		
	12	24	36	12	24	36	12	24	36
Solventless epoxy (2 × 125 µm DFT)									
Wire brushing	0	0	0	2	2	3	2.8/S	3.5/S	2.8/S
Needle gunning	0	0	0	1	1	2	2.8/S	5.5/S	5.2/S
Hydroblasting (Dw2)	0	0	0	0	0	1	6.9/S	7.6/I	8.3/G
Hydroblasting (Dw2 FR)	0	0	0	2	3	3	3.5/I	11.0/I	8.6/I
Hydroblasting (Dw3)	0	0	0	0	0	1	3.5/I	11.0/I	10.7/G
Hydroblasting (Dw3 FR)	0	0	0	0	1	1	4.1/I	8.3/I	11.0/I
Blast cleaning (Sa 2 1/2)	0	0	0	1	2	2	5.5/I	12.4/I	10.3/G
Glass flake epoxy (2 × 125 µm DFT)									
Wire brushing	0	0	10	1	1	3	4.1/S	4.1/S	2.1/S
Needle gunning	0	0	2	2	2	3	2.4/S	5.5/S	8.9/S
Hydroblasting (Dw2)	0	0	0	1	1	1	6.9/G	11.0/I	>17.9/G
Hydroblasting (Dw2 FR)	0	0	0	1	2	2	3.4/G	15.2/G	>17.2/G
Hydroblasting (Dw3)	0	0	0	0	0	1	7.6/G	10.3/I	9.7/I
Hydroblasting (Dw3 FR)	0	0	0	1	1	1	6.9/G	16.9/I	>17.2/I
Blast cleaning (Sa 2 1/2)	0	0	0	0	0	1	6.9/G	13.8/G	13.1/G
Low temperature cure glass flake epoxy (2 × 125 µm DFT)									
Wire brushing	0	0	10	1	1	1	2.8/S	4.6/S	7.6/S
Needle gunning	0	0	12	1	1	2	4.1/S	3.4/S	12.1/S
Hydroblasting (Dw2)	0	0	0	2	2	2	6.9/G	17.2/G	16.6/G
Hydroblasting (Dw2 FR)	0	0	0	2	2	2	5.2/G	14.5/I	11.7/G
Hydroblasting (Dw3)	0	0	0	0	0	1	3.4/G	15.2/G	10.3/G
Hydroblasting (Dw3 FR)	0	0	0	0	1	1	5.5/G	16.9/I	13.8/G
Blast cleaning (Sa 2 1/2)	0	0	0	1	1	2	6.9/G	13.8/G	12.4/G
Modified epoxy (2 × 125 µm DFT)									
Wire brushing	0	0	0	1	1	3	4.8/S	5.5/S	2.8/S
Needle gunning	0	0	0	2	3	3	2.1/S	2.8/S	4.1/S
Hydroblasting (Dw2)	0	0	0	0	0	0	6.9/I	12.8/I	10.3/I
Hydroblasting (Dw2 FR)	0	0	0	1	2	2	3.8/I	11.0/I	8.6/I
Hydroblasting (Dw3)	0	0	0	0	0	1	6.9/I	10.8/I	9.7/I
Hydroblasting (Dw3 FR)	0	0	0	0	0	0	4.1/I	15.2/I	7.9/I
Blast cleaning (Sa 2 1/2)	0	0	0	0	0	1	6.9/I	13.1/I	9.7/G

FR flash rust; Dw surface cleanliness according to STG 2222

^a0 = No cracking; 1 = very slight cracking, no detachment; 2 = slight cracking, no detachment; 3 = moderate cracking, no detachment

^bFailure mode: S = substrate, I = intercoat, G = glue

furnace slag. However, the authors noted an additional effect of the coating to be applied. Chlorinated polyvinyl chloride (PVC), for example, performed especially good if the zinc substrate was blast cleaned.

Table 9.12 lists results of changes in adherence of two coatings on aluminium and steel after 500 h in a condensing water environment as a function of the metal pretreatment process. Although the values for the adhesion are higher in the case of the blast cleaned surface, the behaviour after exposure to water was similar for the

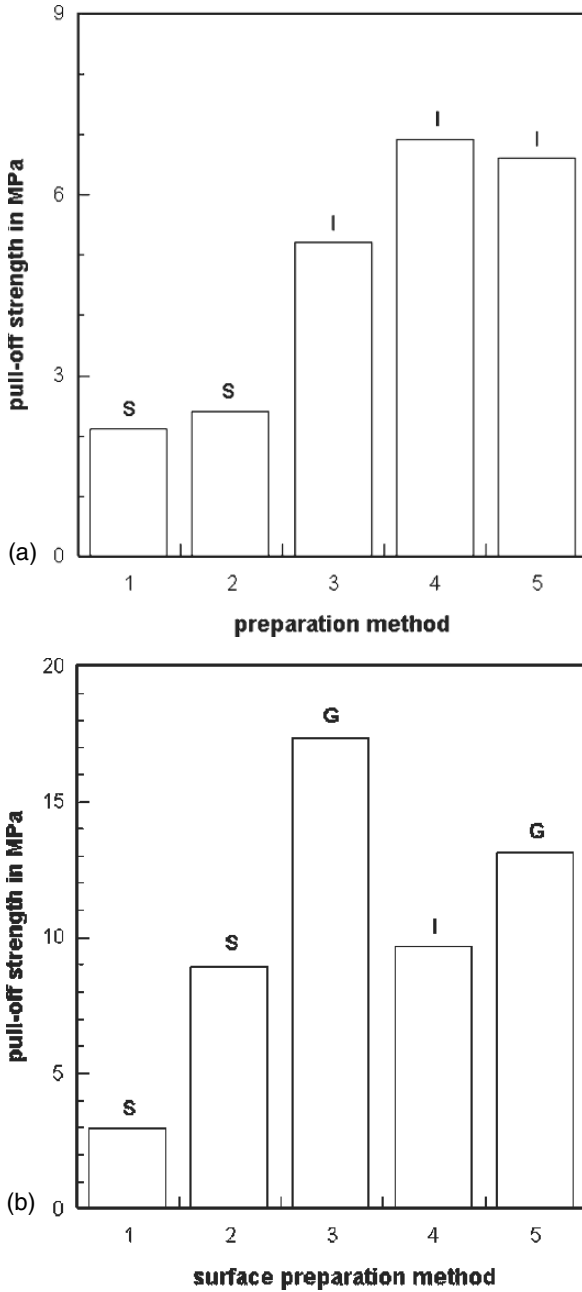


Fig. 9.15 Pull-off strengths after surface preparation-simulated ballast tank conditions. Preparation methods: 1 – hand brush; 2 – needle gunning; 3 – hydroblasting (Dw2); 4 – hydroblasting (Dw3); 5 – dry blast cleaning (Sa 2 1/2); coating thickness: $2 \times 125 \mu\text{m}$. (a) Coal tar epoxy after 24 months (Allen, 1997); (b) Glass flake epoxy after 36 months (Morris, 2000). See Table 9.11 for “S”, “I” and “G”

Table 9.12 Adherence of coatings after 500 h condensation (Leidheiser and Funke, 1987)

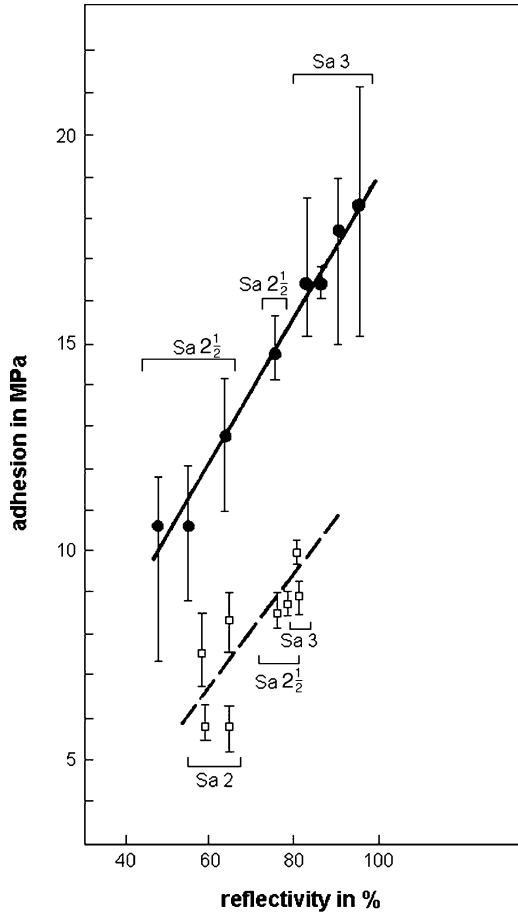
Substrate	Coating	Adhesion before and after water exposure in MPa			
		Degreased		Blast cleaned	
		Before	After	Before	After
Aluminium	Polyurethane	11.4	11.6	27.6	28.2
	Epoxy-polyamide	20.3	22.1	27.6	27.6
Steel	Polyurethane	15.4	3.4	35.9	15.2
	Epoxy-polyamide	19.5	17.4	25.9	21.8

degreased and blast cleaned surfaces. There was very little effect of water exposure for both coatings and for both surface preparation methods in the case of aluminium; both coatings exhibited lower adhesion values after exposure to water for both surface preparation methods in the case of steel.

The effect of cleanliness on the adhesion of thermally sprayed metal coatings to steel substrates is illustrated in Fig. 9.16. Here, substrate cleanliness is characterised through reflectivity. A value of 100% corresponded to the reflectivity of a light grey tile. The higher reflectivity, the higher is surface cleanliness (this relationship holds for a given abrasive material only). It can be seen that high cleanliness promoted high adhesion strength; the relationship was linear for both abrasive types. Another example for the effects of surface cleanliness is illustrated in Fig. 9.17 in terms of surface preparation grade. The relative adhesion of a metal-sprayed coating dropped down to 50%, if the preparation grade was lowered from Sa 3 to Sa 2.

Rider (1987) reported about the bond durability of metals, pretreated with different methods, and adhesives. Wedge style durability tests were conducted, and the durability performance of blast cleaned metallic adherends was compared with standard pretreatments. It was found that blast cleaning at a blasting pressure of $p = 0.45$ MPa led to a notable reduction in the average length of cracks in the adherend-adhesive system. After a root time of 7 h, for example, the crack length was about $l_C = 107$ mm for abrading with distilled water, but it was $l_C = 60$ mm only for blast cleaning. Watts and Dempster (1992), however, who applied wet blast cleaning with aluminium oxide abrasives to adhesively bonded titanium alloys, found that plain blast cleaning did not perform very well; additional preparation steps (anodising and priming) were required to obtain satisfying results. Wedge splitting tests in a corrosive environment were performed by Emrich (2003) for the assessment of adhesion between aluminium substrates and organic adherends. He found that blast cleaning (corundum and glass beads) and subsequent electropolishing reduced the lengths of the cracks in the interface zones between adhesive and substrate compared to samples which were electropolished only. Regarding the two blast cleaning media, the positive effects were stronger for the samples blast cleaned with corundum compared to samples blast cleaned with glass beads. Opposite trends were observed by Emrich (2003) for samples that were blast cleaned and subsequently pickled. In these cases, the pretreatment with corundum and glass beads deteriorated the resistance of the adhesive joint against crack propagation. The shortest crack lengths were measured for the systems where the substrate was pickled only. After an

Fig. 9.16 Effect of substrate cleanliness (reflectivity) on adhesion strength of arc-sprayed aluminium (Bardel, 1974). Parameters: $p = 0.4\text{--}0.6\text{ MPa}$; $d_N = 8\text{--}12\text{ mm}$; $x = 150\text{--}300\text{ mm}$; $\varphi = 60\text{--}90^\circ$. Upper curve: iron grit ($d_p = 100\text{--}900\ \mu\text{m}$), Lower curve: silica sand ($d_p = 600\text{--}1,500\ \mu\text{m}$)



exposure time of about 250h, however, the influence of the surface preparation methods vanished, and the crack length rested on a stable level of about $l_C = 38\text{ mm}$. The author could also prove that the crack length depended on the surface roughness of the profile. A coarse profile (as achieved after blast cleaning and subsequent pickling) delivered longer cracks than a finer profile (as achieved after blast cleaning and subsequent electropolishing). Emrich (2003) also noted that the deformation behaviour of the adhesive in the wedge splitting test had an additional influence on the results. A rather rigid, less deformable adhesive promoted a quick crack extension.

Bardis and Kedward (2002) performed an investigation into the effects of surface preparation methods on the strength of adhesively bonded composite joints. A double cantilever beam (DCB) test was adapted in order to measure the critical strain energy rates (G_{Ic}) of the bonded systems. Results are displayed in Fig. 9.18. Blast cleaned adherends had higher failure loads and higher G_{Ic} -values than non-blast cleaned ones, though the failure mode did not change. Load displacement curves for the bonded composites also depended on preparation method. Emrich (2003)

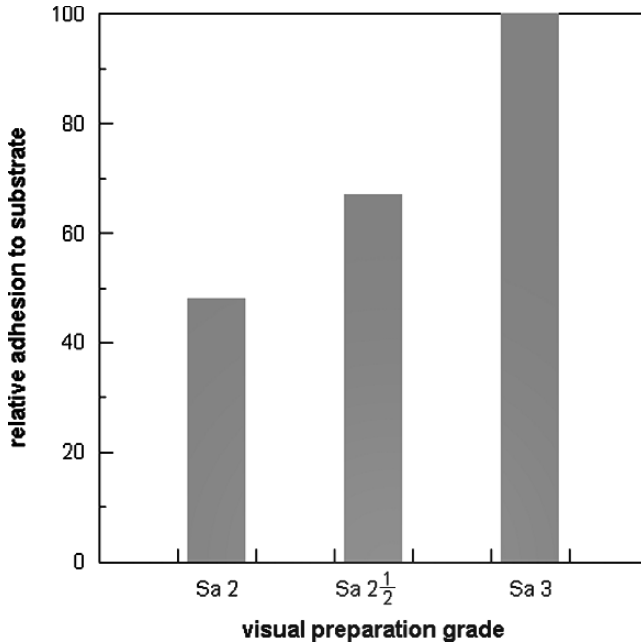


Fig. 9.17 Effects of surface preparation grades on the adhesion strength of metal-sprayed coatings (James, 1984)

estimated the change in the shape of a shear–gliding diagram for adhesive layers. The shear–gliding diagram is comparable with a stress–strain diagram, whereby the stress is replaced by the shear stress, and the strain is replaced by the gliding of the adhesive layer. The results showed that a preparation of the substrate due to blast cleaning (corundum, $p = 0.6$ MPa) and degreasing with acetylene led to a notable change in the shape of the shear–gliding diagram. The use of both methods induced a distinctive drop in shear stress after a number of ten loading cycles in a corrosive medium. However, the shear modulus (ratio between shear stress and gliding) did not change after blast cleaning.

Martin (1997) compared the peel resistance characteristics of pipeline coatings as functions of surface preparation procedures. Results of this study are displayed in Fig. 9.19, which shows results of peel resistance measurements after artificial ageing in a salt spray solution. Blast cleaning could notably improve peel strength, but the level of improvement depended on abrasive type and ageing duration. Aluminium oxide and steel grit delivered very good results, whereas glass beads did not contribute to an improvement in the peel strength. The positive effect of blast cleaning seemed to vanish for long ageing duration; after 16 weeks, the adhesion between coating and substrate was completely deteriorated for the degreased and the glass bead blasted samples. Figure 9.20 illustrates the situation after artificial ageing in a hot water immersion chamber. With the exception of the glass bead blasted samples, the peel resistance curves for the different surface preparation methods ran almost

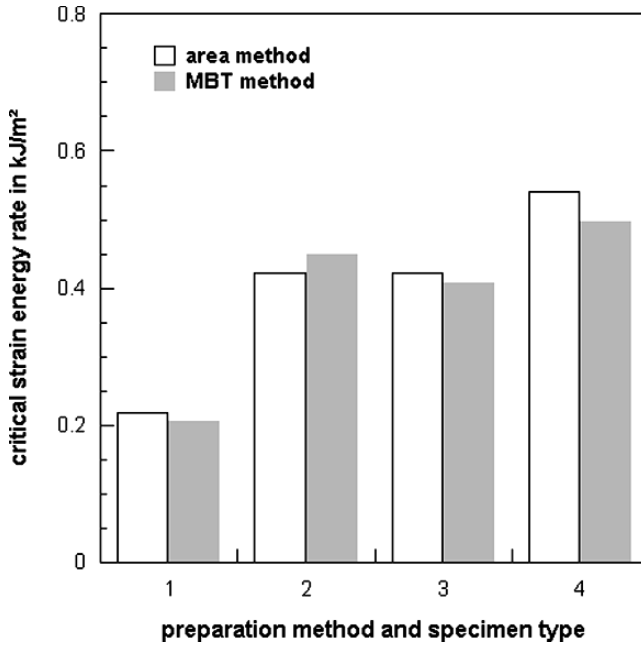


Fig. 9.18 Effect of blast cleaning on the strain energy rate of bonded systems (Bardis and Kedward, 2002). Preparation methods: 1 – RF–RF, no blast cleaning; 2 – RF–RF, blast cleaning; 3 – VB–VB, no blast cleaning; 4 – VB–VB, blast cleaning (RF–RF = release fabric to release fabric orientation; VB–VB = vacuum bag to vacuum bag orientation)

parallel to each other. A gradual reduction in the peel strength with an increase in ageing duration took place. Blast cleaning did not contribute to an improvement in adhesion. However, steel grit showed the best performance among the blast cleaning media in both test situations, and this was contributed to the high roughness at the substrate surface. Substrates with comparative roughness values (glass bead and aluminium oxide) performed quite differently under corrosive environment, and it was concluded that roughness was not the only affecting surface parameter (Martin, 1997). Changes in substrate morphology (contamination) seem to play an important role as well. The worst performance of glass bead can be contributed to the formation of a thin, with Na, Si and Ca, contaminated oxide layer (see Fig. 8.53).

Staia et al. (2000) conducted tests on the adhesion of coatings thermally sprayed on steel substrates. The authors blast cleaned the substrate with aluminium oxide ($d_p = 425\text{--}850\ \mu\text{m}$, $p = 0.34\text{--}0.62\ \text{MPa}$, $\varphi = 75^\circ$) and conducted pull-off tests and interface indentation tests. For the indentation test, they found that critical indentation load, necessary to produce a crack at the interface, as well as the critical length of the crack in the interface between substrate and coating increased if the air pressure increased. Pull-off strength also increased as pressure increased. The authors also found a relationship between air pressure and effects of coating thickness on adhesion. For the rather low air pressure ($p = 0.34\ \text{MPa}$), critical indentation

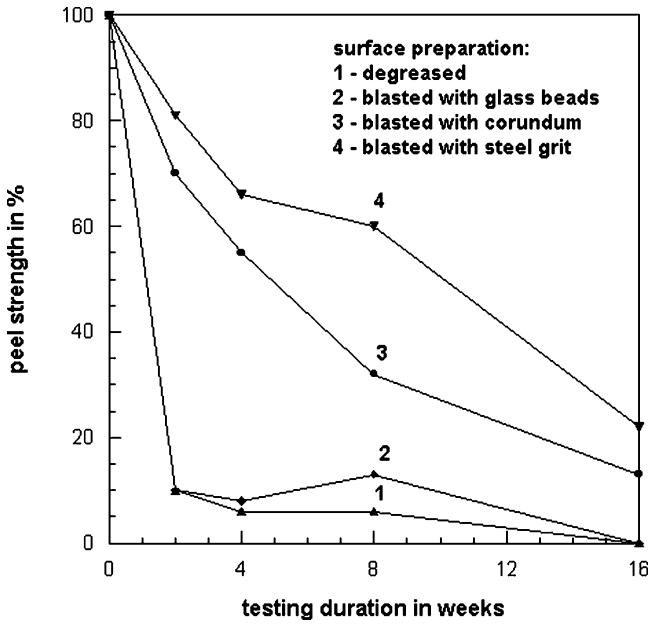


Fig. 9.19 Effects of surface preparation methods on peel resistance of pipeline coatings after salt spray testing (Martin, 1997)

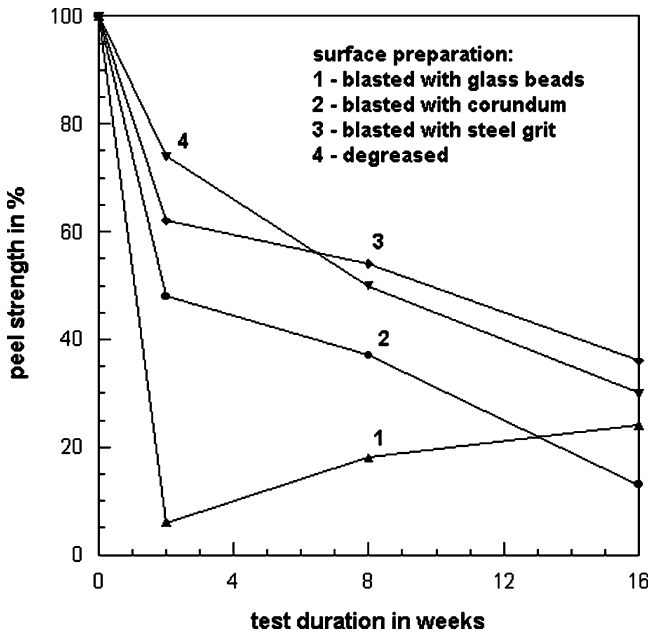


Fig. 9.20 Effects of surface preparation methods on peel resistance of pipeline coatings after immersion tests in 70°C hot water (Martin, 1997)

load depended on coating thickness. This was not the case for the higher air pressures. These results were attributed to the history of residual stress formation in the substrate and the coating material.

Van Rooijen et al. (2005) investigated the effects of chemical and mechanical treatment of steel sheets on the behaviour of fibre–metal laminate (FML). They considered regular steel sheets, molybdenum-enriched steel sheets and aluminium-coated steel sheets. Pretreatment methods were etching and blast cleaning (aluminium oxide, $d_p = 149\text{--}210\mu\text{m}$, $p = 0.2\text{ MPa}$). Peel tests were performed, and it was shown that blast cleaning delivered the highest values for the peel strength (1.62 MPa). The failure mode was cohesive (in the adhesive material) for the blast cleaned samples, which further proved very good adhesion. Etched samples failed at the interfaces between sheet and adhesive; only after a rather long etching time of 3 min, the failure was partially cohesive. Leahy et al. (2003) performed a study into the bonding of fibre reinforced composites to titanium substrates based on a modified wedge test. They deployed blast cleaning (aluminium oxide, mesh 180/220), anodisation, plasma treatment and silicon sputtering as treatment methods. The joints were subjected to 24-hours cycles (wet/dry, cold/hot) for 12 days. The authors reported that a simple blast cleaning was the least successful treatment. The best bond was achieved for the samples treated with a combination of anodisation and subsequent blast cleaning.

Figure 9.21 displays results of furnace cyclic tests on the durability of a multi-layer thermal barrier system. Bond coat surface morphology (not substrate surface

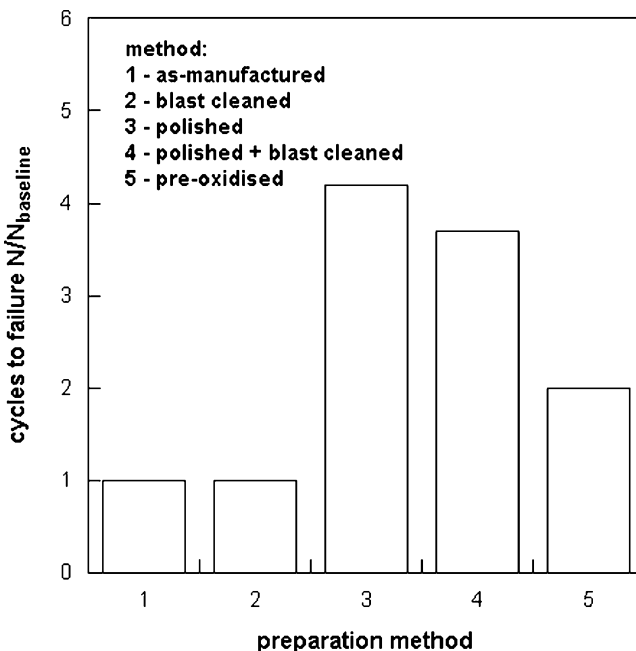


Fig. 9.21 Effects of surface preparation of a bond coat on the failure lifetimes for multi-layer thermal barrier coating systems (Spitsberg et al., 2005). Abrasive type: aluminium oxide

morphology) was varied due to the application of different surface preparation methods, among them combined methods. As the graph clearly shows, the durability was lowest for the systems which were conventionally blast cleaned. Durability could notably be increased if the substrates were treated with a combined method, consisting of polishing and subsequent blast cleaning. Chemical methods also delivered good results. An investigation of the effects of blast cleaning on the durability of thermal barrier coatings (TBS) was also conducted by Xie et al. (2003). The authors blast cleaned a bond coat with aluminium oxide abrasives (grit size 220, $p = 0.2 \text{ MPa}$, $R_z = 75 \mu\text{m}$) and applied a top coat by means of electron beam physical vapour deposition. The lifetime of the coating and the residual stresses in the thermally grown oxide (TGO) were measured as functions of surface morphology. It was found that the lifetime of the system with the blast cleaned bond coat. The lifetime (thermal spallation cycles) of the systems with blast cleaned bond coats varied over a narrow range of 600 to 750 cycles, whereas the systems with the untreated bond coats featured a wide lifetime range of 190 to 1,917 cycles. This result was attributed to the more consistent surface roughness of the blast cleaned bond coat. Another finding was that the stresses in the thermally grown oxides decreased faster if the bond coat was blast cleaned.

Boue (2005) investigated the effect of surface preparation on the adhesion of coatings to bridge ropes and found that blast sweeping delivered results superior to those measured after simple cleaning. Adhesion strength increased after blast sweeping (e.g. from $\sigma_A = 4.1 \text{ MPa}$ after washing to $\sigma_A = 6.6 \text{ MPa}$ after blast sweeping); percentage of cohesive failure also increased if the ropes were blast swept.

Coating type and thickness also determine the effects of surface preparation methods on pull-off strength. Results were provided by Bordeaux et al. (1991). For TiC-coatings, plasma sprayed on inconel substrates, the authors found that pull-off strength was higher for dry blast cleaned substrates (aluminium oxide, $d_p = 7.4 \mu\text{m}$) compared with machined substrates as long as the coating thickness did not exceed a value of $200 \mu\text{m}$. Beyond this thickness value, machined substrates provided better adhesion to the coating. It was also found that the microstructure of the coating was modified if the coating was applied to the machined substrate. Lamellae within the coating were folded due to the rather coarse surface relief. Such foldings resulted in oscillation of the laminations within the coating, which were maximum at the surface and vanished further in the coating.

Loh et al. (2002) found that moisture on the surface of steel substrates affected the adhesion of epoxy to the steel. Results of their measurements are provided in Fig. 9.22. Interface fracture energy steadily degraded with increasing moisture content. For a dry substrate interface, for example, fracture energy was 770 J/m^2 , whereas it was about 50 J/m^2 only for a moisture content of about 8 wt.%.

For bitumen, pull-off strength depends additionally on temperatures of the substrate and the applied bitumen mass; this was shown by Pawlikowski et al. (1966). Pull-off strength increased if steel substrate temperature rose; pull-off strength was four times higher at a steel temperature of 100°C compared with a steel temperature of 20°C . For a given substrate temperature, pull-off strength only slightly increased with a rise in the temperature of the applied bitumen mass.

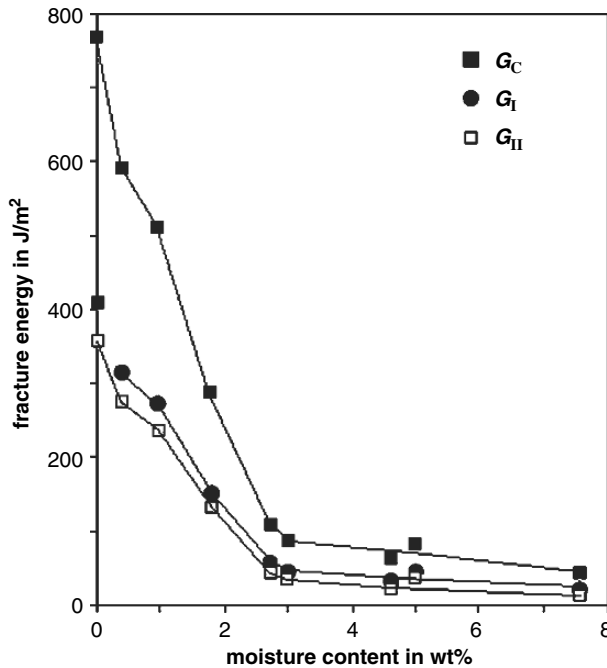


Fig. 9.22 Effect of moisture on the fracture energy of and interface between and epoxy bonded to steel (Loh et al., 2002)

LaBerge et al. (1990) performed tension tests and shear tests to characterise the bond strength of polymer–metal interfaces both for blast cleaned and etched specimens. The Co–Cr substrates were blast cleaned with silica particles ($d_p = 600 - 1,000 \mu\text{m}$), ultrasonically cleaned and then coated with high-density polyethylene (HDPE) powder coatings. The bond strengths for the blast cleaned samples were one order of magnitude lower than those for the etched samples, both for the tension and the shear tests. The authors contributed these results to a high amount of pores in the etched substrates, which promoted interlocking effects between substrate and coating.

Aga and Woldesenbet (2007) investigated the effects of surface preparation on the performance of adhesively bonded graphite/epoxy composites subjected to impact. Although their investigation did not deal with metal substrates, it delivered interesting results in terms of adhesion under impact conditions. The authors performed test with a drop-weight impact machine at different energy levels and estimated the debond areas in the adhesive bond after the testing. The substrate was treated with three surface preparation methods, namely abrading with sandpaper, use of a paper peel plied and blast cleaning ($d_p = 22 \mu\text{m}$, $p = 0.55 \text{ MPa}$). Contact force graphs are shown in Fig. 9.23. The history of the contact forces, but in particular the contact force at the peak of the curves, notably depended on the surface preparation method. The contact force at the peak was highest for the specimen treated with

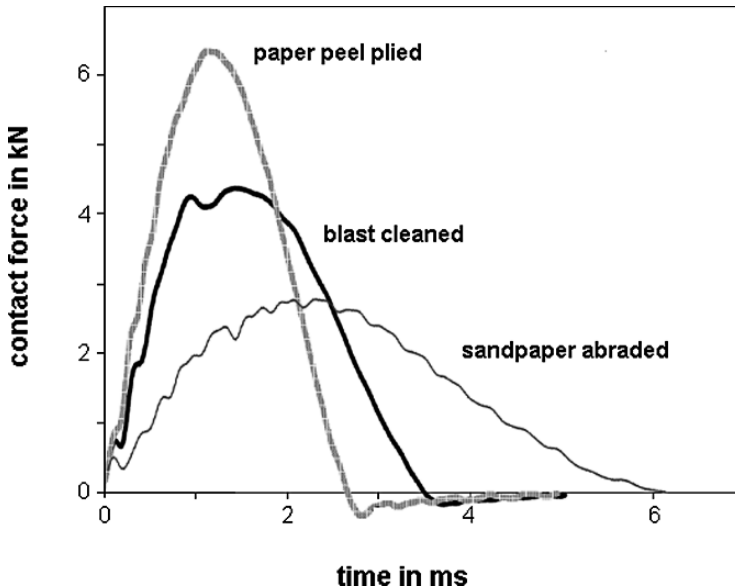


Fig. 9.23 Contact force histories for adhesively bonded graphite/epoxy composite specimens impacted at an energy level of 5.0 J (Aga and Woldeesenbet, 2007)

paper peel plied, followed by blast cleaning and treatment with sandpaper. A somewhat different trend was found for the debond areas after the impact tests. Here, blast cleaned samples delivered the largest debond areas, followed by sandpaper treatment and treatment with paper peel plied. The paper-peel ply surface preparation created the most uniform and smoothest surface. The superior performance of the samples treated with that method was contributed to the formation of very low stress concentrations at the uniform, smooth surface.

Sancaktar and Gomatam (2001) performed tests on the strengths of single lap joints of rolled steel. The strength was measured with a tensile testing machine at different crosshead speeds. Both failure load and ultimate displacement were estimated. The results depicted an effect of the viscosity of the adhesive materials. For a low viscosity adhesive (5–7 Pa s), blast cleaning with aluminium oxide ($p = 0.55$ MPa) generated the highest values for the failure load (4,200 N) as well as for the ultimate displacement (0.013 mm). For a high viscosity adhesive (170–225 Pa s), the maximum value for the failure load was measured for etched adherends. The authors also proved that the loading rate affected the strength parameters. Strength values were always higher for a loading rate of 1 mm/min compared with the values for a loading rate of 100 mm/min. It turned out that the blast cleaned samples were least sensitive to changes in the loading rate. Surface roughness studies of Rider et al. (1999) established that the application of blast cleaning (aluminium oxide, $d_p = 50$ μm , $m_s = 1.2$ g/cm²) increased the fracture energy of an aluminium-epoxy joint exposed to humid conditions by two orders of magnitude. Whereas an ultra-milled aluminium adherend led to a fracture energy of about $G_{Ic} = 5$ kJ/m², the blast cleaned aluminium adherend delivered a fracture

energy of about $G_{Ic} = 20 \text{ kJ/m}^2$ (for a crack velocity of 4 mm/s). Neeb et al. (2000) reported on the performance of adhesive bonds. The substrate was aluminium, and the adhesive was a 2-pack epoxy material. The treatment of the substrate included pickling and blast cleaning ($p = 0.6 \text{ MPa}$, $d_N = 3 \text{ mm}$, $\varphi = 90^\circ$). Abrasive materials were glass beads ($d_p = 100\text{--}200 \mu\text{m}$) and corundum ($d_p = 125\text{--}250 \mu\text{m}$). The adhesion was estimated by means of a wedge test. It was found that the substrate treatment method affected the crack length in the joint. Crack length was highest for the samples blast cleaned with glass beads, and it was lowest for the samples blast cleaned with corundum. The authors contributed these results to the conversion rates of the polymers in the joint. The epoxy applied to the aluminium that was blast cleaned with glass beads showed a high conversion rate and a high final cross-linking density (compare Fig. 9.6). This led to a rather brittle adhesion layer. The epoxy applied to the aluminium that was blast cleaned with corundum, in contrast, showed a low conversion rate (compare Fig. 9.6), and it had a high capability of plastic deformation. Liu et al. (2006) conducted a systematic study into the crack growth in sol-gel treated aluminium/epoxy joints prepared with various methods, namely polishing, etching, sanding and blast cleaning (aluminium oxide, $d_p = 50 \mu\text{m}$, $p = 0.62 \text{ MPa}$). Crack growth velocity and strain energy release rate (respectively fracture energy) were assessed by means of a double cantilever beam in a humid environment. The crack growth velocity for a given energy release rate was highest for the polished samples and lowest for the blast cleaned samples. The energy release rate exhibited a strong dependence on the crack growth velocity, which is a known effect for moisture-assisted crack growth. However, the joints formed with the blast cleaned substrates showed the highest values for the energy release rate ($G_{Ic} = 2,615 \text{ J/m}^2$), whereas the lowest value was found for the joints formed with the polished substrate ($G_{Ic} = 440 \text{ J/m}^2$). Minaki et al. (2007) performed a scratch test in order to assess the adhesion of a plated titanium nitride coat. The substrate was blast cleaned with aluminium oxide ($p = 0.2\text{--}0.4 \text{ MPa}$, mesh 700, $\dot{m}_p = 50\text{--}300 \text{ g/min}$, $\varphi = 90^\circ$, $d_N = 8 \text{ mm}$). The authors found that the critical scratch force increased with an increase in air pressure and in blast cleaning time. This result was attributed to the higher values for profile roughness which was believed to promote a better mechanical bond.

Zhang and Zhou (1997) investigated the effects of blast cleaning on the adhesion of diamond coatings applied to tungsten carbide substrates. The adhesion was evaluated through an indentation test. Flaking of the coatings applied to ground substrates was observed at an indentation load of 600 N, whereas the coatings applied to blast cleaned (alumina, mesh 120 to 500, $p = 0.3 \text{ MPa}$) substrates did not show any flaking until the indentation load reached a value of 800 N.

The delay time between blast cleaning and spraying, respectively coating, has a definite effect on the pull-off strength of coatings. Results of systematic investigations were reported by Apps (1969) for metal-sprayed coatings and by Bullett and Dasgupta (1969) for organic coatings. The results of the authors revealed that the pull-off strength notably dropped for longer delay times if the substrates were exposed to an open environment. A drop in pull-off strength could be prevented if the blast cleaned substrates were stored in a desiccator (Apps, 1969).

9.2.3 Blast Cleaning Parameters Effects on Adhesion

9.2.3.1 Effects of Blasting Angle

Process parameters also affect adhesion of coatings to substrate. Apps (1969, 1974) and Berndt and Lin (1993) reported about effects of blasting angle and abrasive type on the adhesion of metal-sprayed aluminium coatings. For all situations, optimum values for maximum adhesion could be found at rather high impact angles. In many cases, the optimum blasting angle was at $\varphi = 90^\circ$, but the correct location of the certain optimum angle was affected by the abrasive type. Some results of these investigations are listed in Table 9.13. Amada et al. (1999) found, for aluminium oxide coatings, very low adhesion strengths at low blasting angles, whereas, adhesion was maximum at a blasting angle of $\varphi = 79^\circ$. Ishikawa and Tobe (2003) noted a sensitive relationship between blasting angles and spraying angles. Results of their study are displayed in Fig. 9.24. If both parameters were effectively related to each other, maximum adhesion strength could be achieved. Differences in adhesion strength for different parameter configurations were as high as 300%.

9.2.3.2 Effects of Abrasive Type, Size and Shape

Bahlmann (1982) found that the relative adhesion of organic coatings to steel substrates increased from a value of 1.00 for untreated steel to a value of 1.30 for blast cleaning with round steel grit, and to a value of 6.4 for blast cleaning with irregular chilled casting. Therefore, both hardness and particle shape notably affected adhesion. Similar relationships were reported by James (1984) for thermally sprayed coatings (see Table 9.14). Apps (1974) noted a strong influence of coating thickness on adhesion strength. If, for example, an aluminium coating exceeded a thickness of 200 μm , adhesion to the substrate started to drop. This drop was highly pronounced if copper slag and chilled iron grit were used for blast cleaning, but less important if aluminium oxide abrasive was used.

Varacalle et al. (2006) performed a systematic study into the effects of abrasive types on the pull-off strengths of aluminium, sprayed on a low-carbon steel substrate. Their results, partly listed in Table 9.15, depicted a strong effect. Steel grit delivered the highest adhesion values, whereas chilled iron grit provided the lowest

Table 9.13 Effects of blasting angle and abrasive type on the adhesion of aluminium coatings (Berndt and Lin, 1993); optimum blasting angle designates angles for maximum adhesion strength

Abrasive type	Optimum blasting angle in $^\circ$
New chilled iron grit	90
Used chilled iron grit	90
Worn chilled iron grit	90
Round shot	20
Alumina grit	60
New copper slag grit	40
Worn copper slag grit	30 and 90

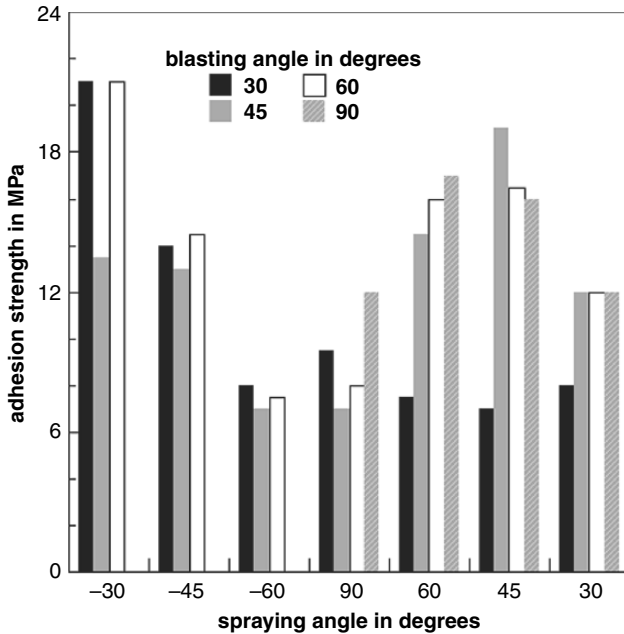


Fig. 9.24 Effects of blast cleaning angle and spraying angle on the adhesion of a metal-sprayed coating (Ishikawa and Tobe, 2003)

pull-off strength values. It is obvious from these studies, that the abrasive type must be adjusted to both substrate and coating properties in order to provide maximum adhesion.

Mannelqvist and Groth (2001) reported about the influence of abrasive type on the adhesion of adhesive epoxy joints to stainless steel panels. Results of their study are displayed in Fig. 9.25. Joint tensile strengths of samples blast cleaned with an irregular abrasive (grit) were notably higher than strengths of samples that were blast cleaned with glass beads. Feist et al. (1988) reported about the effects of numerous abrasive materials on the adhesion of sprayed metal coatings to steel; results are plotted in Fig. 9.26. It can be seen that the abrasive type had a notable

Table 9.14 Effect of abrasive type and coating application on relative adhesion of flame-sprayed zinc and aluminium (James, 1984)

Abrasive	Relative adhesion in %			
	Aluminium		Zinc	
	Arc-sprayed	Flame-sprayed	Arc-sprayed	Flame-sprayed
G 12/24	100	33	28	31
Slag	36	31	23	25
Sand ($d_p = 0.6-1.5$ mm)	72	16	18	17
Sand ($d_p = 0.1-1.0$ mm)	54	-	22	20

Table 9.15 Effect of abrasive type on the adhesion of sprayed aluminium to blast cleaned low-carbon steel (Varacalle et al., 2006)

Abrasive type	Pull-off strength in MPa
Steel grit HG-16	8.21
Steel grit HG-18	8.07
Steel grit HG-25	7.82
Steel grit HG-40	8.48
Copper slag	6.83
Coal slag	7.07
Chilled iron grit	3.62

influence on the pull-off strength values. Even for equal roughness values (say $R_z = 50 \mu\text{m}$), pull-off strength of sprayed aluminium dropped from $\sigma_A = 10 \text{ MPa}$ for basalt or furnish slag to $\sigma_A = 4 \text{ MPa}$ for nickel slag. Similar was the situation for a roughness of $R_z = 80 \mu\text{m}$. Yankee et al. (1991) could also show that abrasive type can play a decisive role in adhesion. For equivalent roughness values and equal cleaning procedures, it was the profile characteristics (thus, the abrasive shape), that determined the adhesion strength. These effects are illustrated in Fig. 9.27. Blast cleaning with aluminium oxide delivered notably higher adhesion strengths. The distinct profile characteristics generated during the blast cleaning with aluminium

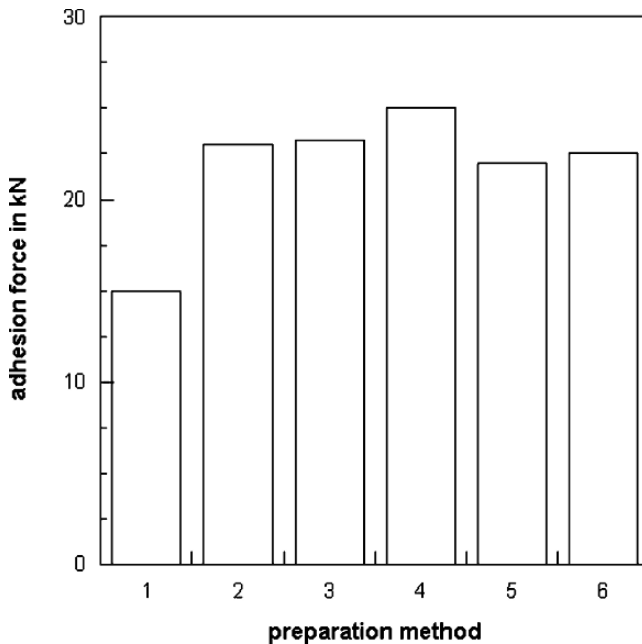


Fig. 9.25 Effects of surface preparation methods on the adhesion of adhesive epoxy joints to steel (Mannelqvist and Groth, 2001). Preparation methods: 1 – degreasing; 2 – Scotch-Brite; 3 – steel brushing; 4 – blast cleaning with grit; 5 – blast cleaning with glass beads; 6 – water blasting

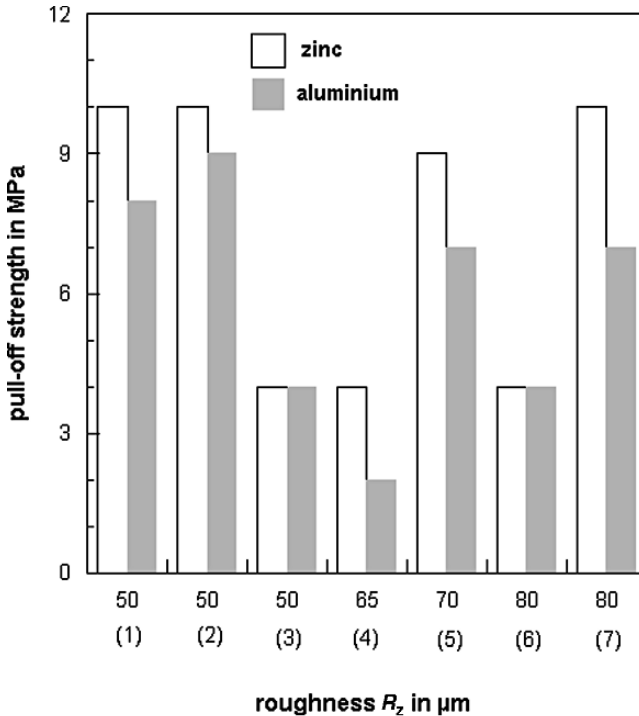


Fig. 9.26 Effects of abrasive materials on the adhesion of metal-sprayed coatings to steel (Feist et al., 1988). Abrasive types: (1) – basalt; (2) – furnace slag; (3) – VV-slag; (4) – electric-furnace slag; (5) – nickel–iron slag; (6) – lead–tin slag. Parameters: $p = 0.6$ MPa; $d_p = 630\text{--}1,250$ μm ; $d_N = 8$ mm; nozzle type: Laval nozzle

oxide seemed to promote a good bond of the thermally sprayed hydroxylapatite coating to the titanium substrate. However, as also shown in Fig. 9.27, intense post-cleaning of the substrate surfaces with ultrasound reduced the differences in adhesion strength, which pointed to additional contamination effects (see Sect. 8.5.3). Brewis et al. (1999) could prove that the preparation of aluminium substrates with carbon dioxide particles (“dry ice blasting”) could notably improve the strength of single-lap shear joints. Joint strength increased from 1,859 N for a degreased surface up to 4,420 N for carbon dioxide blast cleaned surfaces.

Apps (1967) found that the individual influence of the abrasive type to the adhesion of thermally sprayed coatings depended on the blasting angle. Results of his study are plotted in Fig. 9.28. The effect of abrasive deterioration, for example, is much more distinguished if the abrasives were propelled at normal angle. At this angle, even worn steel grit performed better than steel grit that was just used once.

Tests performed on the adhesion of enamel coatings to steel by Sorokin et al. (1977) verified notable effects of particle shape. Steel shot abrasives delivered better bonding conditions than steel grit particles. The coatings were unevenly distributed

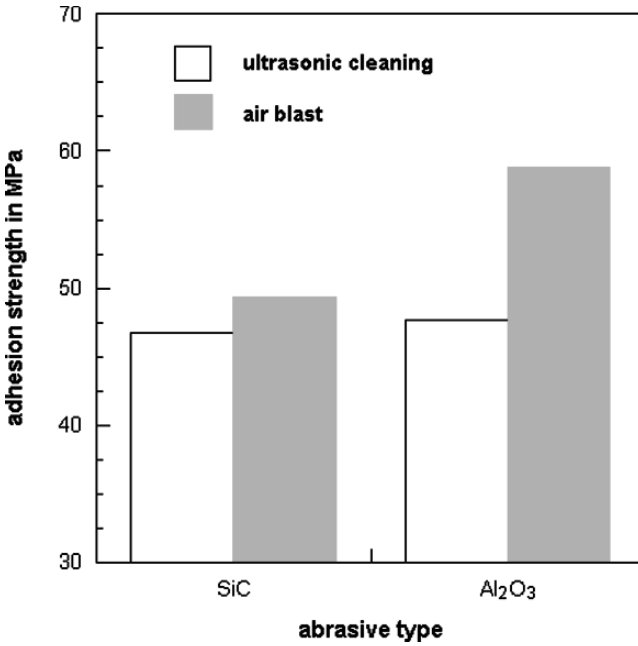


Fig. 9.27 Effects of abrasive type and substrate fine-cleaning on the adhesion of a plasma-sprayed coating to titanium (Yankee et al., 1991)

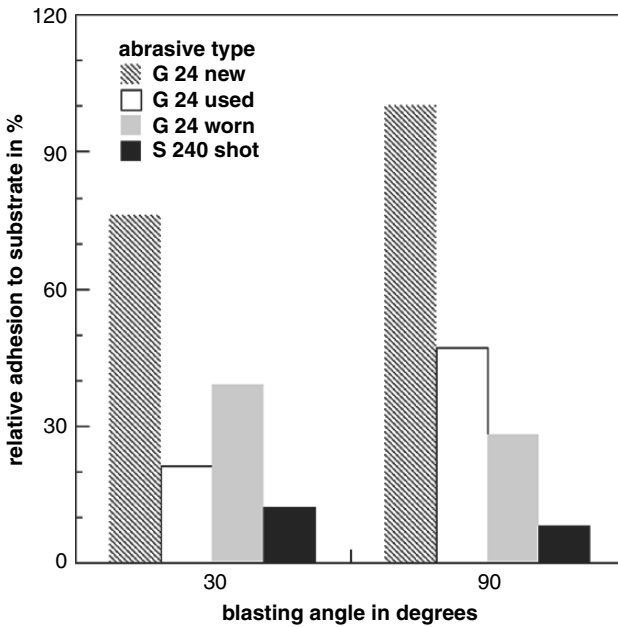


Fig. 9.28 Effects of blasting angle and abrasive quality on the relative adhesion strength of thermally sprayed coatings (Apps, 1967)

over the grit blasted surfaces and peeled during application. Beitelman (2003) applied the abrasive shape designations according to Fig. 2.8 and measured the adhesion performance of organic and metallic coatings to the prepared substrates. Results of this study are provided in Table 9.16. Abrasive particle shape had an influence on the adhesion strength of the metallic coatings, whereas it was insensitive to the adhesion strength of the organic coating. This difference in the coating types was also found for the failure behaviour during the adhesion tests. Particle shape affected the failure type for the metal-sprayed coating, but not that of the organic coating. The amount of cohesion failure of the metal-sprayed coating dropped with a decrease in the angularity of the abrasive particles.

9.2.3.3 Effects of Air Pressure

Apps (1969) performed a systematic study into the effects of blasting pressure variations on the adhesion of metal-sprayed coatings to steel substrates. Although the author noted a certain trend that adhesion increased with an increase in blasting pressure, blasting pressure did not always show a distinct relationship to the adhesion of coatings to steel substrates. An example is illustrated in Fig. 9.29. It seemed that optimum blasting pressure ranges existed which depended on abrasive quality. Worn abrasive materials deteriorated adhesion strength. Sofyan et al. (2005) found an increase in bond between WC-Co coatings and steel if blast cleaning pressure increased.

9.2.3.4 Effects of Stand-off Distance

Apps (1969) performed a systematic study into the effects of changes in stand-off distance on the adhesion of metal-sprayed coatings on steel plates and steel bars, and he did not find any notable trends. The pull-off strength was unaffected by variations in the stand-off distance in the range between $x = 15$ and 90 mm.

9.2.3.5 Statistical Assessment Models

Day et al. (2005) and Varacalle et al. (2006) performed statistical analyses into the effects of numerous process parameters on the adhesion of thermally sprayed coatings to steel substrates. Day et al. (2005) derived the following relationship:

Table 9.16 Abrasive shape effects on the adhesion of coatings to blast cleaned substrates (Beitelman, 2003)

Particle shape ^a	Pull-off strength in MPa		Cohesion failure in %		Adhesion failure in %	
	Organic ^b	Metallic ^c	Organic	Metallic	Organic	Metallic
Very angular	13.3	9.8	100	81	0	19
Angular	13.2	9.4	100	83	0	17
Sub-angular	13.0	9.7	100	86	0	14
Sub-rounded	13.3	8.8	100	45	0	55
Rounded	13.3	8.3	100	44	0	56

^aCrushed steel grit (G-59); see Fig. 2.9 for shape designations

^bZinc-rich organic coating (DFT = 93–130 μm)

^cMetal-sprayed Zn/Al (DFT = 340–500 μm)

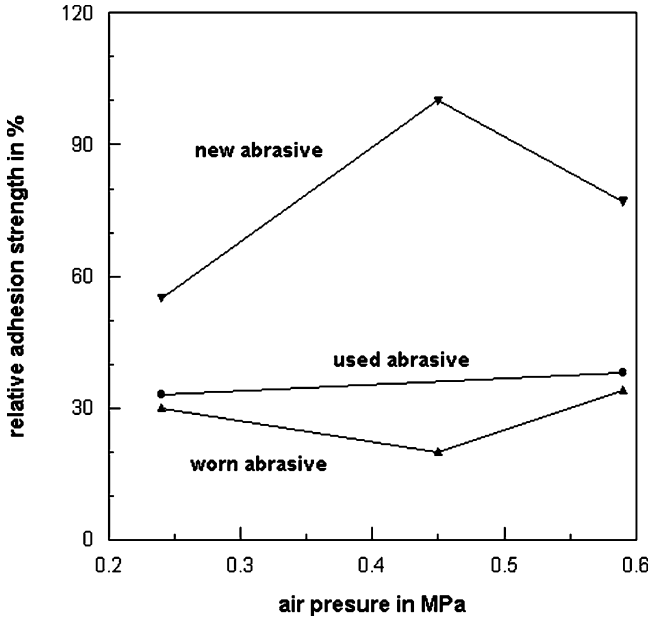


Fig. 9.29 Effects of air pressure and abrasive type on the adhesion of adhesive epoxy joints to steel (Mannelqvist and Groth, 2001)

$$\sigma_A = 38.7 \cdot GN + 76.9 \cdot p + 414.2 \cdot n_s + 182.6 \cdot x + 20.6 \cdot \phi \quad (9.4)$$

In this equation, the adhesion strength is given in psi, the grit number is given in mesh, the pressure is given in psi, the stand-off distance is given in), and the blasting angle is given in degrees. Varacalle et al. (2006) derived the following relationship for aluminium, sprayed on a low-carbon steel substrate:

$$\sigma_A = 3,518.2 + 457.3 \cdot x + 59.55 \cdot C_G + 8.6 \cdot p_S - 13.78 \cdot x^2 - 0.113 \cdot C_G^2 - 0.012 \cdot p_S^2 \quad (9.5)$$

In that equation, the adhesion strength is given in kPa, the stand-off distance is given in cm, the spray pressure is given in kPa, and the spray gun current is given in A. The equation holds for the use of HG 16 steel grit ($d_p = 1,000\text{--}1,700\ \mu\text{m}$).

9.3 Mechanical Behaviour of Coatings

Surface preparation methods can affect the mechanical behaviour of coatings, mainly those of sprayed metal or ceramic coatings. Examples are provided in Fig. 9.30. In the two graphs, four sections can be distinguished as functions of coating thickness and power density: (1) fusion of the inconel substrate, (2) segmentation

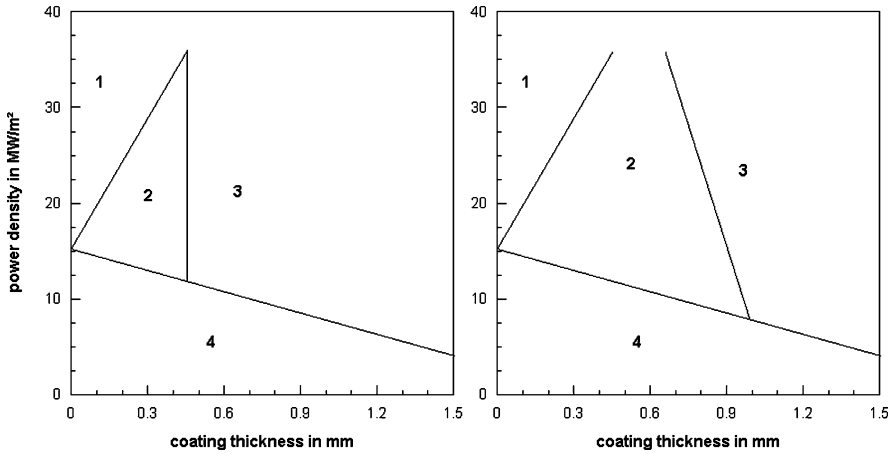


Fig. 9.30 Effects of surface preparation methods on coating failure types during thermal shock tests (Bordeaux et al., 1991). Left: blast cleaning; right: macro-roughening; Failure types: 1 – substrate fusion; 2 – segmentation of coating; 3 – delamination; 4 – no damage

of the coating, (3) delamination and (4) no damage. The no-damage region was not notably affected by the surface preparation method, but the coatings were more sensitive to segmentation if blast cleaning was performed. For blast cleaning, the limit for segmentation was at a coating thickness of about 400 μm , whereas it was at a coating thickness of about 950 μm for the machined substrate. These relationships are of importance for the application of thermal barrier coatings.

Sobiecki et al. (2003) measured the microhardness of tungsten carbide coatings applied to substrates which were prepared with different surface preparation methods, but they did not record any effect.

Bochenin (2005) performed investigation on aluminium coatings deposited by diffusion metallisation on steel substrates. The abrasive material used was iron shot ($d_p = 1,000 \mu\text{m}$); the air pressure was $p = 0.6 \text{ MPa}$. The coated specimens were placed into a furnace, heated to 1,000°C and held for 90 h. The specific weight loss of the coating was defined as a measure for its heat resistance. It was found that heat resistance of the coating could be affected notably due to blast cleaning of the substrate. The heat resistance depended on several blast cleaning parameters. Results are displayed in Fig. 9.31. For the stand-off distance, an optimum value could be detected, whereas heat resistance was highest for a perpendicular blast cleaning angle.

Tolpygo et al. (2001) investigated the behaviour of thermal barrier coatings deposited on (Ni, Pt) Al bond-coat substrates. The samples were cyclically oxidised. Each cycle consisted of 10 h of exposure at 1,150°C, with heating and cooling rates of about 200°C/min. The authors noted that blast cleaning of the substrate with aluminium oxide particles promoted a very high growth rate of the oxide scale. The high oxidation rate was explained by impurities from the blast cleaning

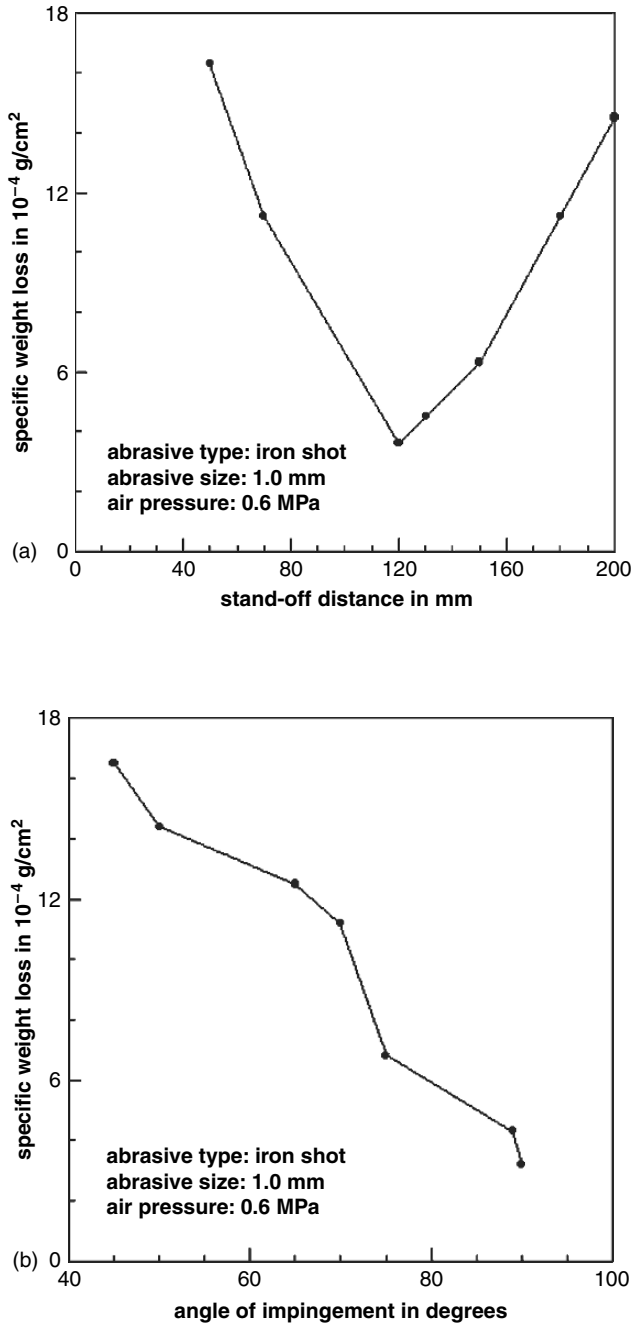


Fig. 9.31 Effects of blast cleaning parameters on the heat resistance of aluminium coatings deposited to a steel substrate (Bochenin, 2005). (a) Effect of stand-off distance; (b) Effect of blasting angle

process (alkali and titanium), which became incorporated into the growing scale and significantly accelerated the oxide growth. The high grow rate resulted in cracking and spalling of the scale followed by a mass decrease after only 30 ten-hour cycles at 1,150°C. The scale formed on the aluminised surfaces had much lower impurity content and a slower growth rate, and they showed an excellent spalling resistance during cyclic oxidation. Based on these results, blast cleaning is expected to have a detrimental effect on the durability of thermal barrier coatings.

A study into the performance of sol-gel-derived coatings over blast cleaned aluminium alloys was conducted by You et al. (2001). The substrate was blast cleaned with aluminium oxide powder ($d_p = 20$ and $100 \mu\text{m}$). The authors found that the coating layer was more uniform for the sampled blast cleaned with the finer abrasives. These coatings also showed a smaller number of cracks after firing compared with the coatings applied over the substrate blast cleaned with the coarser abrasives. The authors attributed these results to effects of substrate roughness.

9.4 Corrosion Protection Performance of Coatings

The corrosion protection performance of organic coatings can be evaluated by means of electrochemical methods. One method that became notably involved in coating testing during the recent years is EIS. The physical and chemical background is complex and beyond the scope of this book. The reader may refer to Baboian (1986). One assessment parameter, however, is the electrical resistance of a coating. If this parameter has high values, corrosion protection capability of the coating is high as well. Studies where effects of different surface preparation methods on the corrosion protection performance of coatings were investigated by means of EIS were conducted by Lin et al. (1992), Santaga et al. (1998), Vesga et al. (2000) and Elsner et al. (2003). Lin et al. (1992) investigated the effects of surface preparation methods on the electrical resistance of rather thin organic coatings. Results of their study are plotted in Fig. 9.32. It appeared that for the coating systems studied, blast cleaning deteriorated the performance of the coatings. The authors contributed this result to areas of “deficient” coating coverage (e.g. peaks of a rough substrate), which occurred at the blast cleaned surfaces.

Figure 9.33 shows results of EIS measurements performed by Vesga et al. (2000) on organic primers applied to blast cleaned steel substrates. The primer behaviour was subdivided into three stages, denoted “R” (resistive), “CR” (capacitive/resistive) and “C” (capacitive) in Fig. 9.33. The value for the resistance at a given time can indicate the state of the primer degradation. The lower this value, the more severe degradation took place. It can be seen that the resistance had rather low values for the primer applied to the wet blast cleaned steel. The resistance of the primer applied to the dry blast cleaned steel was one order of magnitude higher. It was demonstrated that the pore resistance of the primers showed the same qualitative trend over the

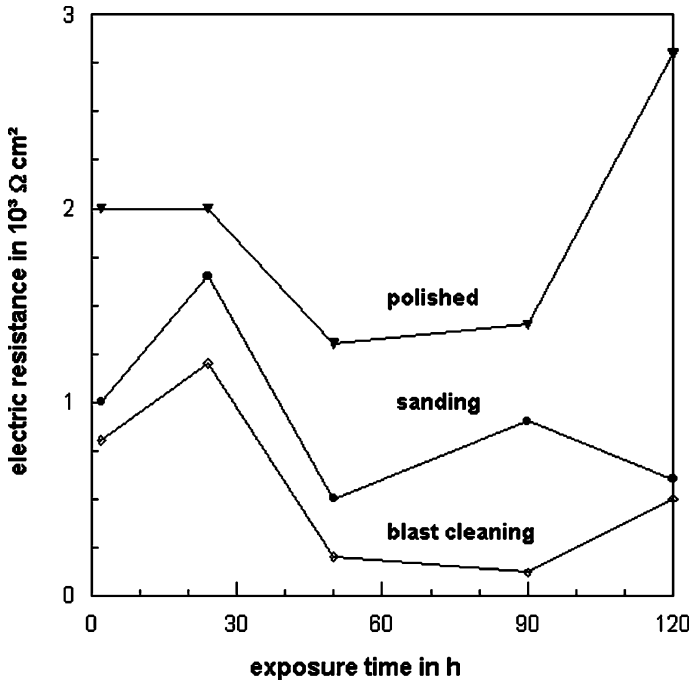


Fig. 9.32 Effects of surface preparation methods on the corrosion protection performance (electric resistance) of thin organic coatings (Lin et al., 1992). Coating: epoxy; substrate: cold-rolled steel; parameters: $p = 0.7$ MPa; $d_p = 150\text{--}300$ μm ; abrasive material: sand

exposure time as the *KIV*-value (see Fig. 9.3). Thus, the resistance seemed to be indicative of the corrosion protective performance of the primer. It can further be seen from the graphs in Fig. 9.33 that the resistive status (“R”) was reached after a shorter period of time for the primer applied to the wet blast cleaned steel substrate. In the status “R”, the primer may swell excessively and irreversibly, taking up extra water and ions from the electrolyte and may be damaged. Vesga et al. (2000) observed that the primer lost adhesion to the substrate in that stage.

Cambruzzi et al. (2005) utilised EIS for the assessment of abraded coating systems. The background of this study is that paint inspectors sometimes claim that a well-adhering primer coat must not be removed during coating repair applications. If this strategy is being followed, the primer is, if not removed, however abraded by the impinging particles. Cambruzzi et al. (2005) applied a special abrasion test to a polyester powder coating and measured the electric resistance after a variety of abrasion cycles. The results shown in Fig. 9.34 depicted a notable deterioration of the corrosion protection performance of the coating. In less than 300 cycles, almost all samples reached values lower than the protection threshold of 10^6 $\Omega\text{ cm}^2$. It was observed that the abrasive particle size played an important role in the reduction of the protective properties of the coatings, since the most severe conditions were observed for the coarsest grains.

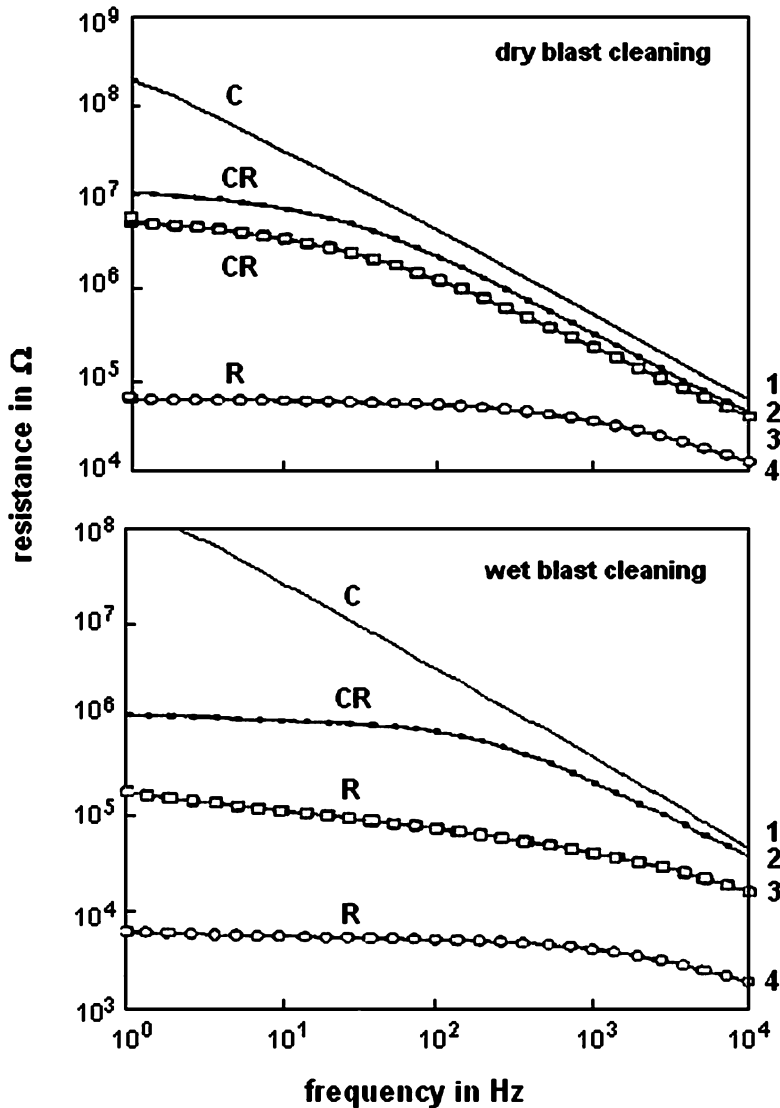


Fig. 9.33 Bode and Nyquist plots for an organic primer applied to blast cleaned steel substrates (Vesga et al., 2000). 1 – initial condition; 2 – after 180 h; 3 – after 360 h; 4 – after 860 h

9.5 Deposition and Transport Phenomena

The deposition rate of a coating is actually not a performance parameter of an already existing coating, but it may affect the behaviour of the final coating. The relationships between deposition rate and blast cleaning processes are not well understood. Heya et al. (2005) performed an investigation in the deposition rate of

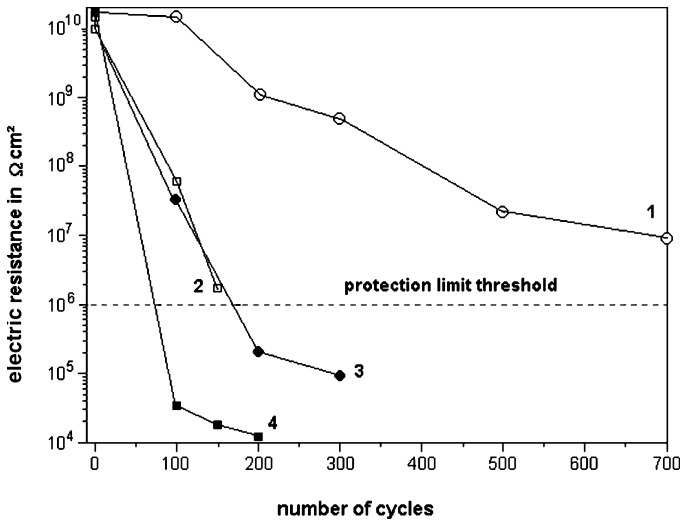


Fig. 9.34 Effects of abrasion damages on the corrosion protection performance (electric resistance) of an organic powder coating (Cambruzzi et al., 2005). Abrasive parameters: 1 – mesh 20–69, 250 g; 2 – mesh 12–20, 250 g; 3 – mesh 20–60, 1000 g; 4 – mesh 12–20, 1000 g)

SiN_x-films on tungsten wires in catalytic chemical vapour deposition (Cat-CVD). If a high deposition rate is required for this process, the temperature is usually increased which is accompanied with a rise in electric power consumption. Heya et al. (2005) blast cleaned the wires with silicon carbide particles with sizes between 10 and 20 μm, and they measured the deposition rates. For a given electric power of 70 kW, the deposition rate increased from about 9 nm/min for untreated wires to 12 nm/min for blast cleaned wires. This result was explained with the higher specific surface of the blast cleaned wires, which was about 35% higher than that of untreated wires.

Another effect worth noting is the influence of profile parameters on the carburisation of turbine blades as witnessed by Locci et al. (2004). Blast cleaning with coarse aluminium oxide provided a more efficient surface condition for carburisation compared with machining and polishing. This effect could directly be contributed to the corresponding surface roughness values. Carbide depth after a 2-hour standard carburisation process was, for example, 33 μm for a roughness of $R_a = 0.34 \mu\text{m}$, but it increased up to 85 μm for a roughness of $R_a = 1.7 \mu\text{m}$.

9.6 Wire Embedment in Polymer Matrices

A special case is the treatment of metal wires, which become embedded in a polymer matrix. The performance of such a reinforced structure depends to a great amount on the bond between steel and matrix. Jonnalagadda et al. (1997)

Table 9.17 Effect of surface preparation on the adhesion between metal wires and a polymer matrix (Jonnalagadda et al., 1997)

Surface preparation of the wires	Interfacial bond strength in MPa	Max. wire displacement in μm	Max. shear stress induced in the matrix in MPa
Untreated	10.5	0.14	5.5
Blast cleaned	30.3	0.11	8.9
Hand sanded	9.0	0.31	4.0
Acid etched	8.1	0.32	4.1

performed investigations into the mechanical contact behaviour of nickel–tungsten wire steels (wire diameter: $150\mu\text{m}$) embedded into a commercial polymer material. The authors utilised different methods for the surface preparation of the wires, including acid etching, blast cleaning and sanding. They estimated interfacial bond strength, wire displacement under load and shear stresses induced in the matrix by means of pull-out tests, interferometry and photoelasticity. Results of these studies are listed in Table 9.17. Blast cleaning significantly increased the bond strength, whereas sanding and acid etching actually reduced the interface strength. Blast cleaning resulted in lower wire displacement and higher interfacial stresses.

9.7 Coating Formation Processes

9.7.1 Spreading and Splashing

The formation of splats from impinging liquid metal or ceramic drops can be accompanied by flattening effects. During flattening, molten material flows radially at high speed, while cooling and possibly solidification of the particle/substrate interface takes place. The first sprayed coating particles, which impinge the substrate, hit a profiled surface that considerably affects the flattening process. Flattening can be characterised by a flattening degree, which is the ratio between final splat diameter and initial splat diameter. It is defined as follows (Moreau et al., 1995):

$$\frac{D_S}{D_0} = f_F \cdot \left(\frac{v_D \cdot \rho_C \cdot D_0}{\eta_C} \right)^{0.2} \quad (9.6)$$

In this equation, D_S is the final splat diameter, D_0 is the initial splat diameter, v_D is the velocity of the impinging drop, ρ_C is the coating material density and η_C is the coating material dynamic viscosity. Figure 9.35 illustrates the effects of different surface preparation methods on the flattening degrees of plasma-sprayed molybdenum on a molybdenum substrate. The flattening degree tended to decrease if substrate roughness increased. It seemed that the constant f_F in (9.6) is a function of

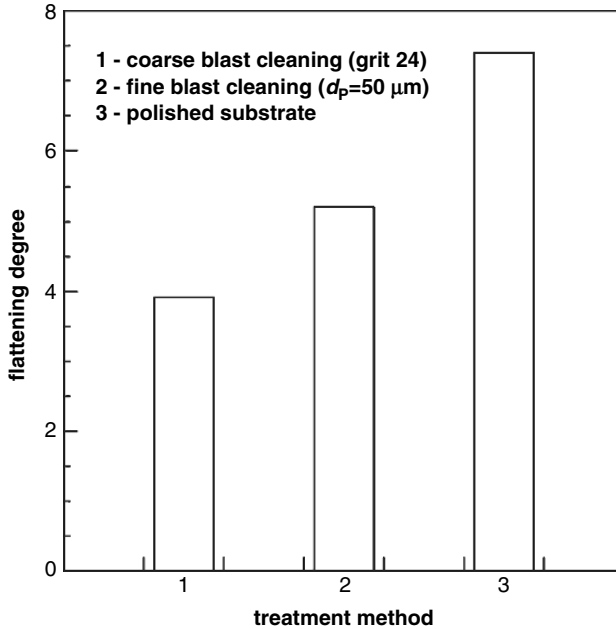


Fig. 9.35 Effects of surface preparation on the flattening degree of plasma-sprayed molybdenum particles (Moreau et al., 1995)

the surface preparation method. It has lower values for the methods which produce rougher surfaces, such as blast cleaning with coarse aluminium oxide particles. Moreau et al. (1995) also found that the surface preparation method affected splat surface and flattening time. The smoother the substrate, the larger the splat surface and the longer the flattening time. The cooling time, in contrast, was found to be longer if the surface was blast cleaned with the coarse aluminium oxide.

Ma et al. (2006) studied the effect of the roughness (R_a) of blast cleaned substrates on the splat formation of HVOF-sprayed tungsten carbide. The results showed that with an increase in roughness, the restriction to flattening was enhanced in a way that the number of spherical to nearly spherical splats reduced, whereas the number of splats with complex morphologies increased.

Liu et al (2006) conducted a study on the spreading kinetics of a wetting liquid for different surface preparation methods, namely polishing, etching, sanding and blast cleaning (aluminium oxide, $d_p = 50 \mu\text{m}$, $p = 0.62 \text{ MPa}$). The substrate was aluminium, and the wetting liquid was hexadecane. Results of their investigations are provided in Fig. 9.36. The relationship between spread radius and time followed a power law:

$$\frac{D_S}{\lambda} \propto t^{k_D} \tag{9.7}$$

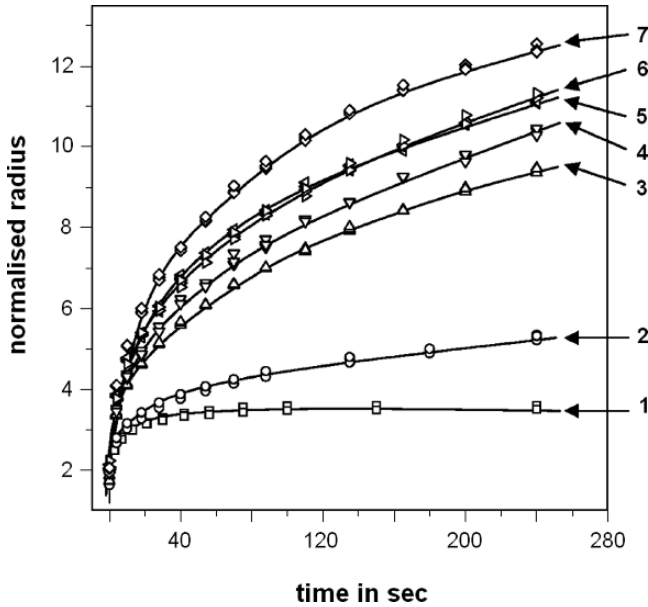


Fig. 9.36 Effects of surface preparation methods on the spreading kinetics of hexadecane on aluminium (Liu et al., 2006). Preparation methods: 1 – polishing; 2 – etching; 3 – sanding (mesh 240); 4 – sanding (mesh 180); 5 - sanding (mesh 120); 6 – blast cleaning; 7 – blast cleaning and subsequent etching. Normalized radius is ratio between spread radius and (drop volume)^{1/3}.

The power exponent k_D was a function of the surface preparation methods. Values for the power exponent are listed in Table 9.18. It can be seen that blast cleaning substrates provided the highest values.

9.7.2 Powder Solidification

Sobolev et al. (2000) conducted a study into the solidification of a WC-Co powder during the high-velocity oxygen-fuel spraying on a copper substrate. They generated two roughness levels on the substrate: smooth due to polishing; rough due to blast cleaning. The authors analysed a number of process parameters of the solidification process, namely solidification rate, cooling rate, thermal gradient, crystal size and

Table 9.18 Spreading kinetics power exponent k_D for different surface preparation methods (Liu et al, 2006)

Surface preparation method	k_D -value
Polishing	0.11
Etching	0.16
Sanding (mesh 240 to 120)	0.27
Blast cleaning (aluminium oxide, $d_p = 50 \mu\text{m}$, $p = 0.62 \text{ MPa}$)	0.29

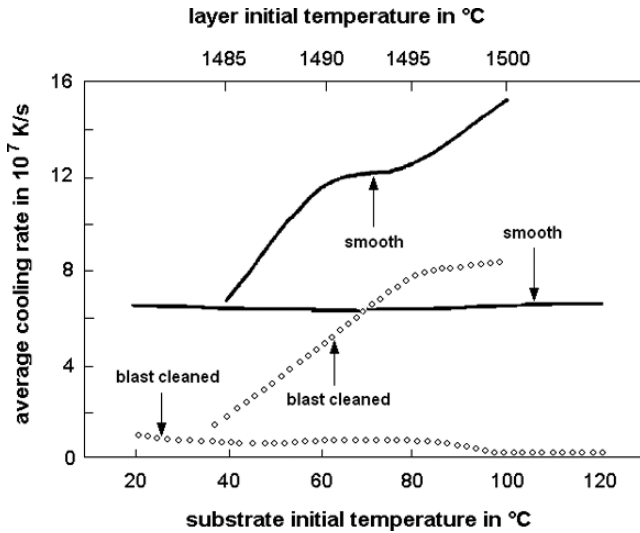


Fig. 9.37 Relationship between solidification rate, initial temperature and surface preparation (Sobolev et al., 2000)

intercrystalline distance. An example is provided in Fig. 9.37. It can be seen that the cooling rate was lower if the powder was sprayed on the blast cleaned substrate. The same trend was found for the thermal gradient and for the solidification rate. The authors also calculated the contact heat transfer coefficient for the substrate-coating interface, and they reported the following values: $6.6 \cdot 10^6 \text{ W}/(\text{m}^2 \cdot \text{K})$ for the polished substrate and $3.33 \cdot 10^6 \text{ W}/(\text{m}^2 \cdot \text{K})$ for the blast cleaned substrate. The basic result was that a rough (blast cleaned) substrate allowed more time for forming a good bond to develop a strongly adherent coating. These results are good examples on how blast cleaning can affect the coating formation process in its very early stage.

9.7.3 Nucleation Processes

Zhang and Zhou (1997) found a relationship between the nucleation density of diamond applied to tungsten carbide and the surface preparation method. It was found that blast cleaning provided the highest nucleation density. The authors related this result to the morphology of the blast cleaned substrate (skewness between -1 and -3 ; compare Fig. 8.53) which provided a suitable contact angle for diamond nucleation.

Machu (1963) discussed the effect of surface treatment on the phosphating process of steel. He pointed out that, from the point of view of electro-chemistry, a high number of activated pits (local anodes) at the steel surface is one preposition

for an efficient phosphating process. The number and the energy state of these pits determine number of crystal nuclei, nucleation rate and crystal growth. Such active pits will be created during mechanical pre-treatment, including blast cleaning. As a result, very fine-grained, thin and corrosion protective phosphate layers are being formed on the steel substrate after blast cleaning.